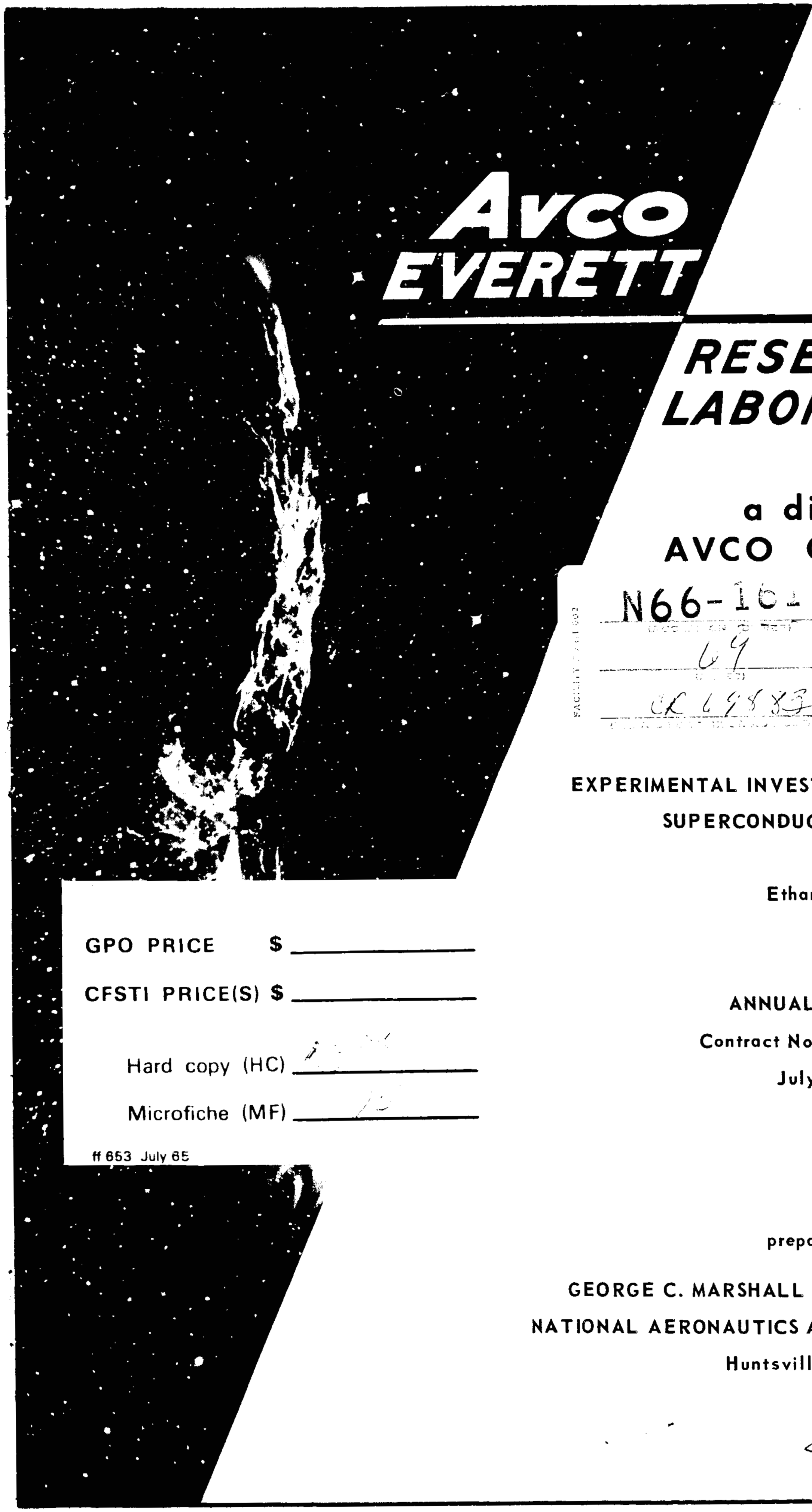

AVCO EVERETT RESEARCH LABORATORY

a division of
AVCO CORPORATION

N66-16?8? | 1
64 | 23
CR 64883

EXPERIMENTAL INVESTIGATION OF ADVANCED SUPERCONDUCTING MAGNETS

Ethan Hoag

GPO PRICE $ __________

CFSTI PRICE(S) $ __________

Hard copy (HC) __________

Microfiche (MF) __________

ff 653 July 65

ANNUAL REPORT

Contract No. NAS 8-5279

July 1965

prepared for

GEORGE C. MARSHALL SPACE FLIGHT CENTER
NATIONAL AERONAUTICS AND SPACE ADMINISTRATION
Huntsville, Alabama

S/ 35568-K

EXPERIMENTAL INVESTIGATION OF ADVANCED SUPERCONDUCTING MAGNETS

by

Ethan Hoag

ANNUAL REPORT

AVCO-EVERETT RESEARCH LABORATORY
a division of
AVCO CORPORATION
Everett, Massachusetts

Contract No. NAS 8-5279

July 1965

prepared for

GEORGE C. MARSHALL SPACE FLIGHT CENTER
NATIONAL AERONAUTICS AND SPACE ADMINISTRATION
Huntsville, Alabama

TABLE OF CONTENTS

I. INTRODUCTION

The use of superconducting coils in large systems has been retarded by the fact that the design of superconducting magnets has been more of an art than a straightforward application of physics and engineering principles with the subsequent evolution of a predictable coil design. Superconducting coils have been designed up to the present using mainly data obtained from similar coils. The problem of scaling data to coils of different sizes and shapes was a formidable one and when building a coil of a type that had not previously been built, its performance could not be predicted--sometimes within 50%. This situation is tenable when dealing with small coils; however, it becomes intolerable in large coil systems where the investment in materials and labor can be considerable.

Recently, however, it has been shown that superconducting coils can be stabilized.[1] Stabilization achieves two results. First, the short sample current carrying capacity is consistently achieved in coils with no size or shape effects. Second, the uncontrolled transition to the normal state with the resultant loss of liquid helium and magnetic field is eliminated. These two results combine to allow superconducting coils to be designed and built with the assurance that their performance will have no more uncertainty in it than the usual engineering tolerances.

Although this work was verified by tests on a wire coil, the implications are equally valid for coils with other conductor shapes provided the peculiarities unique to them are taken into account.

Superconducting strip does in fact have unique properties which present problems that must be overcome before a successful stabilized coil can be constructed from it. It is a major purpose of this effort to solve these problems and construct a coil which can be used to verify the stabilization theory for strip superconductors and refine it.

The major problems unique to strip superconductors are as follows:

1) Anisotropy
2) Truncation in wide samples
3) Joints to and between superconductors
4) Fabrication of stabilized conductors in lengths suitable for coil construction.

All of these problems have been overcome as a result of the present effort and a successful coil has been constructed and tested. This work was confined almost entirely to the study of Nb-25% Zr strip since it is the most readily available and widely used of all materials currently available. The following is a summary description of this work.

II. STABILIZED CONDUCTORS

The behavior of a superconductor in a coil or as part of a circuit is determined by its terminal characteristics. These terminal characteristics are in general a function of the magnetic field and the relative degree to which the superconductor is cooled.

A superconducting material exposed to an external magnetic field can be characterized as having zero resistance up to its critical current. At this point the voltage rises very sharply at practically constant current. This in turn results in the Joule heating raising the temperature of the superconductor.

Due to the high current densities characteristic of superconductors, the current must usually be considerably reduced before the sample can again cool down and return to fully superconducting behavior. The return to the superconducting state can be made at higher currents if an alternate path of low resistance is provided and the conductor is well cooled.

The analysis presented here concerns the behavior of a short sample of superconductor which has been stabilized by placing it in good electrical and thermal contact with a normally conducting substrate exposed to the liquid helium bath and in an externally applied magnetic field. Consider what must happen in such a conductor as the current is increased. At low currents, all the current flows in the superconductor until it reaches its maximum current carrying capacity. If the conductor is well cooled so that the conductor temperature rise can be neglected, then a further increase in current will result in a "spilling over" of the excess current from the superconductor to the normal substrate.

The net result is a sharing of the total current between the superconductor and the substrate. The superconductor must develop some resistance to limit its current, otherwise it would take on more current. Obviously, if not enough cooling is provided, the temperature rise due to current in the substrate will result in a lowering of the current carrying capacity of the superconductor resulting in more current in the substrate and a complete transfer of current to the substrate may occur.

To determine the stability of the conductor we must analyze the behavior of the conductor when current is shared between the substrate and the superconductor. To do this in a general fashion, we shall include a heating per unit length of q_h.

If we define $0 \leq f \leq 1$ as being the fraction of the total current I which flows in the substrate, then the voltage per unit length of the conduction is:

$$v = \rho I f / A \qquad (1)$$

where ρ and A are the resistivity and cross sectional area of the substrate.

$$T - T_b = \frac{vI + q_h}{hP} = \frac{\rho I^2 f}{hPA} + \frac{q_h}{hP} \tag{2}$$

where h is the heat transfer per unit surface area per unit temperature rise from the conductor to the cooling bath at a temperature T_b and is assumed to be a constant. The perimeter of the conductor that is exposed to the cooling bath is P.

Under conditions of current sharing between superconductor and substrate, the temperature T, and the externally applied magnetic field determine the current in the superconductor.

Let us define $I_{ch}(T_b)$ as the maximum current a superconductor can carry at the bath temperature T_b and in an externally applied magnetic field, H. This is the so-called short sample or H-I curve of the superconductor. Since the current in the superconductor I_s is given by

$$I_s/I_{ch} = g[(T - T_b) / (T_{ch} - T_b)] \tag{3}$$

it follows that $g(0) = 1$ and $g(1) = 0$. Here T_{ch} is the superconductor critical temperature in a field H and g represents the functional relationship between the superconductor current and temperature. For most superconductors[2] the functional relationship is well approximated by a straight line:

$$I_s/I_{ch} = [1 - (T - T_c) / T_{ch} - T_b)] \tag{4}$$

It is useful to introduce a stability parameter.

$$\alpha \equiv \frac{\rho I_{ch}^2}{hPA (T_{ch} - T_b)}$$

Use of Eqs. (1) and (2) and the defining of α result in the following expressions after some simplification:

$$f = \frac{(I/I_{ch}) - 1 + Q_h}{(I/I_{ch})[1 - \alpha (I/I_{ch})]} \tag{5}$$

$$vA/\rho I_{ch} = \frac{(I/I_{ch}) - 1 + Q_h}{1 - \alpha (I/I_{ch})} \tag{6}$$

$$(T - T_b) / (T_{ch} - T_b) = \frac{\alpha I/I_{ch} (I/I_{ch} - 1 + Q_h}{I - \alpha (I/I_{ch})} + Q_h \tag{7}$$

where $$Q_h = \frac{q_h}{hP(T_{ch} - T_b)}$$

Equations (5), (6) and (7) are shown plotted in Figs. 1, 2, and 3 respectively for several values of α. For $Q_h = 0$ and for several values of Q_h for $\alpha = 2$.

Figure 2 shows the voltage-current characteristics of a unit length of the conductor. Since we are interested in the behavior of this conductor in a coil which is inductive, we should examine the stability at constant current.

Two distinct types of operation are possible for no heat input ($q_h = 0$) depending on the value of α. For $\alpha < 1.0$ no voltage appears until $I = I_{ch}$ (the superconductor current carrying capacity). For $I > I_{ch}$ the voltage increases gradually with current. The characteristic is everywhere single valued. For $\alpha > 1.0$ the operation is more complicated:

For: $$0 < I \leq \frac{I_{ch}}{\sqrt{\alpha}}$$

Single valued operation results with all the current in the superconductor ($v = 0$).

For: $$\frac{I_{ch}}{\sqrt{\alpha}} \leq I \leq I_{ch}$$

Double valued operation results with either all the current in the superconductor or all the current in the substrate.*

* Operation on the negative resistance part of the curve is unstable for a constant current type of operation.

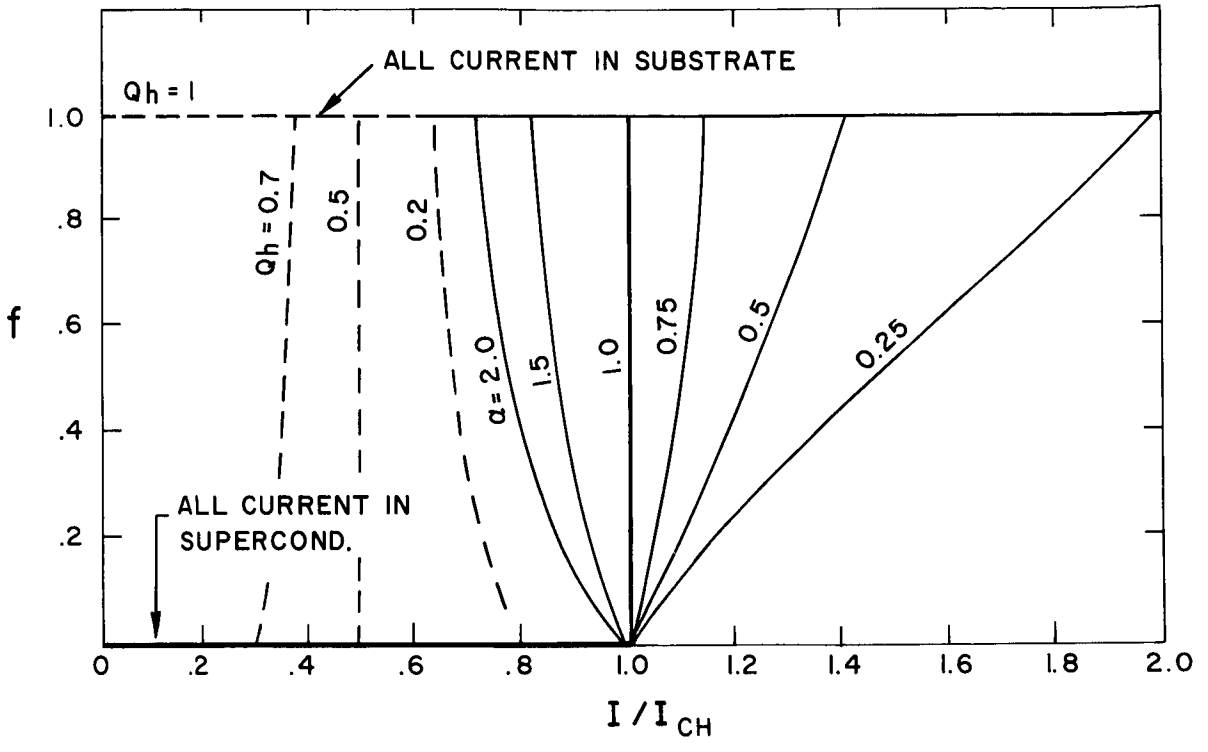

Fig. 1 Current sharing between a stabilized superconductor and a cooled substrate. The dependent variable f is the fraction of the total current conducted by the substrate.

A4042

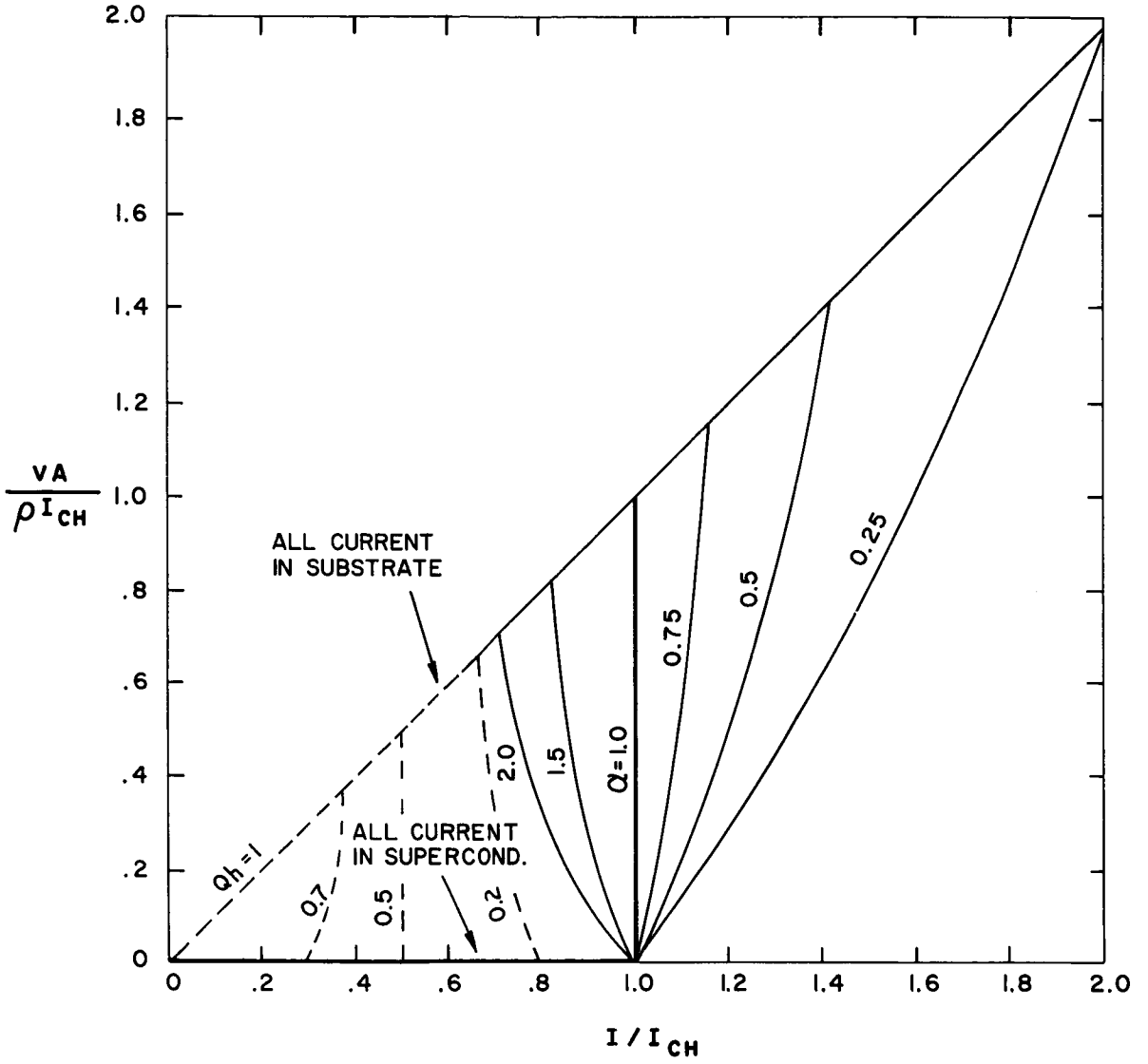

Fig. 2 Voltage - current characteristics for a stabilized superconductor - substrate combination.

A3527 X

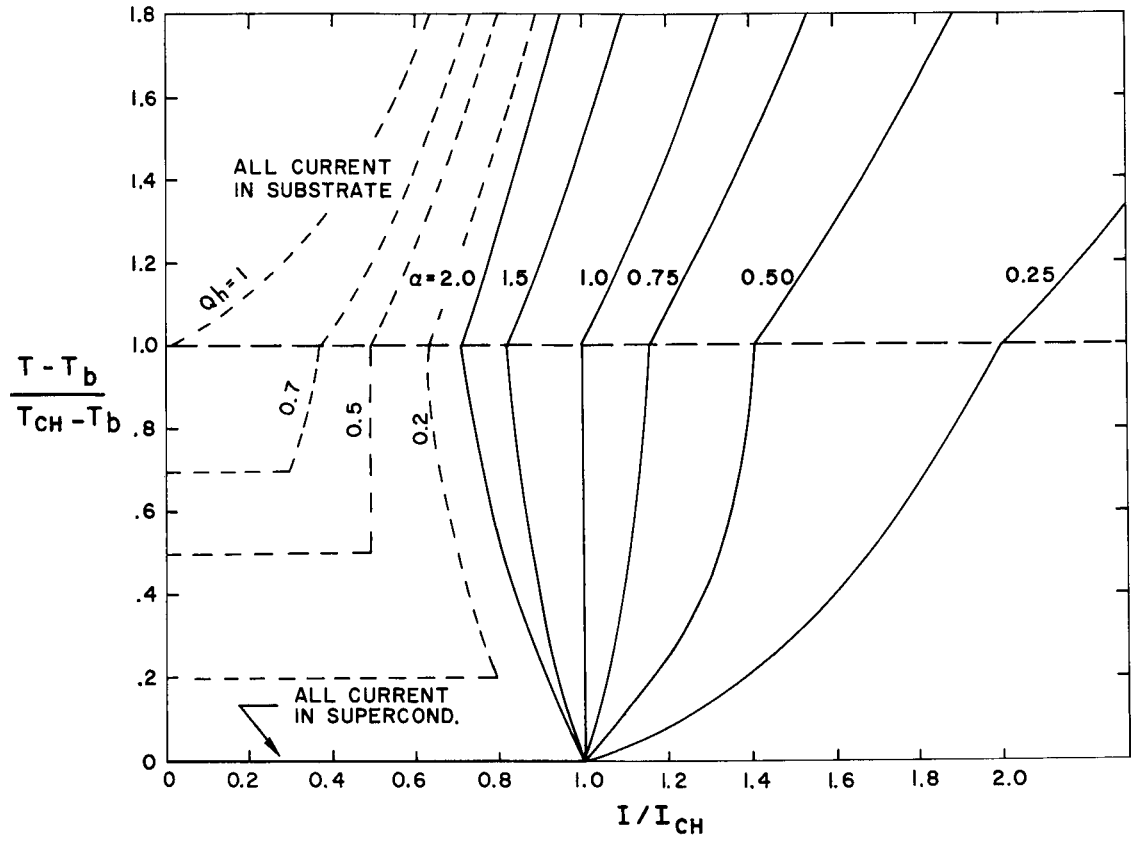

Fig. 3 Temperature rise of a stabilized superconductor as a function of current and cooling parameter.

For: $I > I_{ch}$

Single valued operation results with all the current in the substrate.

Completely stable operation results for $\alpha \leq 1.0$. For $\alpha > 1.0$ stable operation is limited to currents up to $I_{ch}/\sqrt{\alpha}$. In the region of current above $I_{ch}/\sqrt{\alpha}$ steady operation with all the current is still possible up to I_{ch}; however, should the conductor suffer a disturbance then all the current will immediately switch to the substrate.

The effect of heat is easily summarized by the following behavior:

1) Current begins to transfer out of the superconductor at a total current of

$$\left.\frac{I}{I_{ch}} = 1 - Q_h\right] \quad f = 0+$$

which simplifies to $I/I_{ch} = 1$ for $Q_h = 0$. If $Q_h = 1.0$ then a voltage exists for all values of $I/I_{ch} > 0$. The physical interpretation of this is that enough heat is supplied to raise the temperature to its critical value even with no current flowing. This means that the range of interest is $0 < Q_h < 1.0$.

2) The amount of heat necessary to completely drive the current out of the superconductor at any current is:

$$\left.Q_h\right] = 1 - \alpha \left(\frac{I}{I_{ch}}\right)^2$$

$$f \quad \square \quad 1.0$$

3) The slope of the voltage-current characteristic at the first appearance of voltage is:

$$\left.\frac{d\,(vA/\rho I_{ch})}{d\,(I/I_{ch})}\right] \quad v = 0+ \quad = \quad \frac{1}{1 - \alpha\,(1 - Q_h)}$$

since α is multiplied by $(1 - Q_h)$ the effect of heat is to reduce the slope of the voltage-current curve at the first appearance of voltage. However, this is done at the expense of lowering the current at which voltage first appears.

To illustrate this behavior Figs. 1, 2 and 3 show the voltage-current characteristics as a function of heat input parameter Q_h, for $\alpha = 2.0$.

III. ANISOTROPY AND ITS REDUCTION BY ANNEALING

The anisotropy of critical current density with respect to magnetic field direction in Nb-Zr rolled strip is well-known and has been reported on by many authors. It is generally agreed that the underlying causes of this anisotropy lies with the unique metallurgical structure induced by the rolling rather than by the shape ot the sample tested.[3-11] Experiments involving certain annealing procedures designed to reduce anisotropy in Nb-25% Zr rolled strip have borne out this opinion.

Two sets of samples similar to that shown in Fig. 4 were sheared from 0.051 mm thick Nb-25% Zr cold rolled strip. Each of these samples was annealed for different lengths of time at temperatures of 560 and 700°C and at a pressure of approximately 10^{-4} torr., as set forth in Table I.

Table I

Sample No.	Annealing Temperature (°C)	Time at Temperature (hours)
A46	700	0.12
A48	700	0.25
A49	700	0.50
A41	700	1.00
A31	560	1.00
A39	560	3.00
A34	560	6.00
A38	560	15.0

Samples were tested in the field of a stantionary Helmholtz type superconducting magnet capable of producing up to 4 T.[12] They were energized by means of an external dc current source and the onset of the normal state was detected by means of a microvoltmeter connected across the necked down test section. Anisotropy data was obtained by rotating the sample with respect to the magnet so as to vary the orientation angle, Θ, as defined in Fig. 4.

Typical results, showing how the anisotropy curve for the unannealed material is modified by the annealing process is shown in Fig. 5. As seen there the peak current at low orientation angles is effected very little whereas that at the high angles is greatly increased.

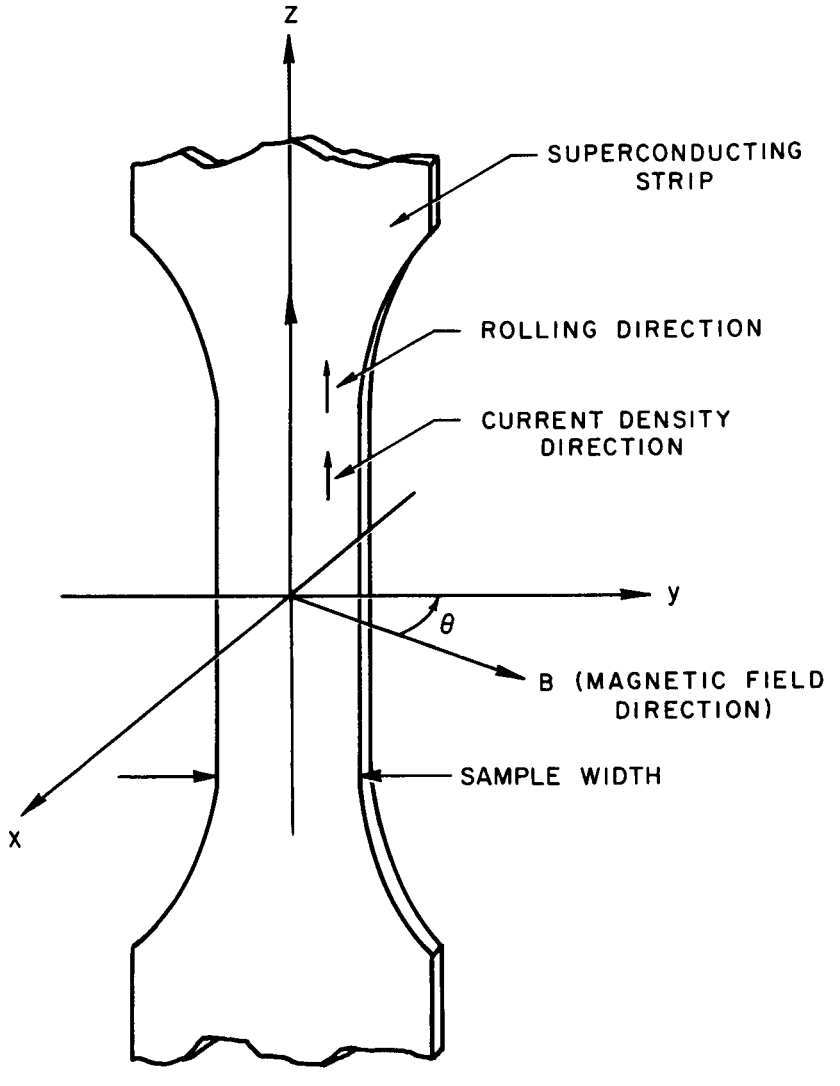

Fig. 4 Typical example of short sample showing relationships between strip geometry, rolling plane and magnetic field orientation.

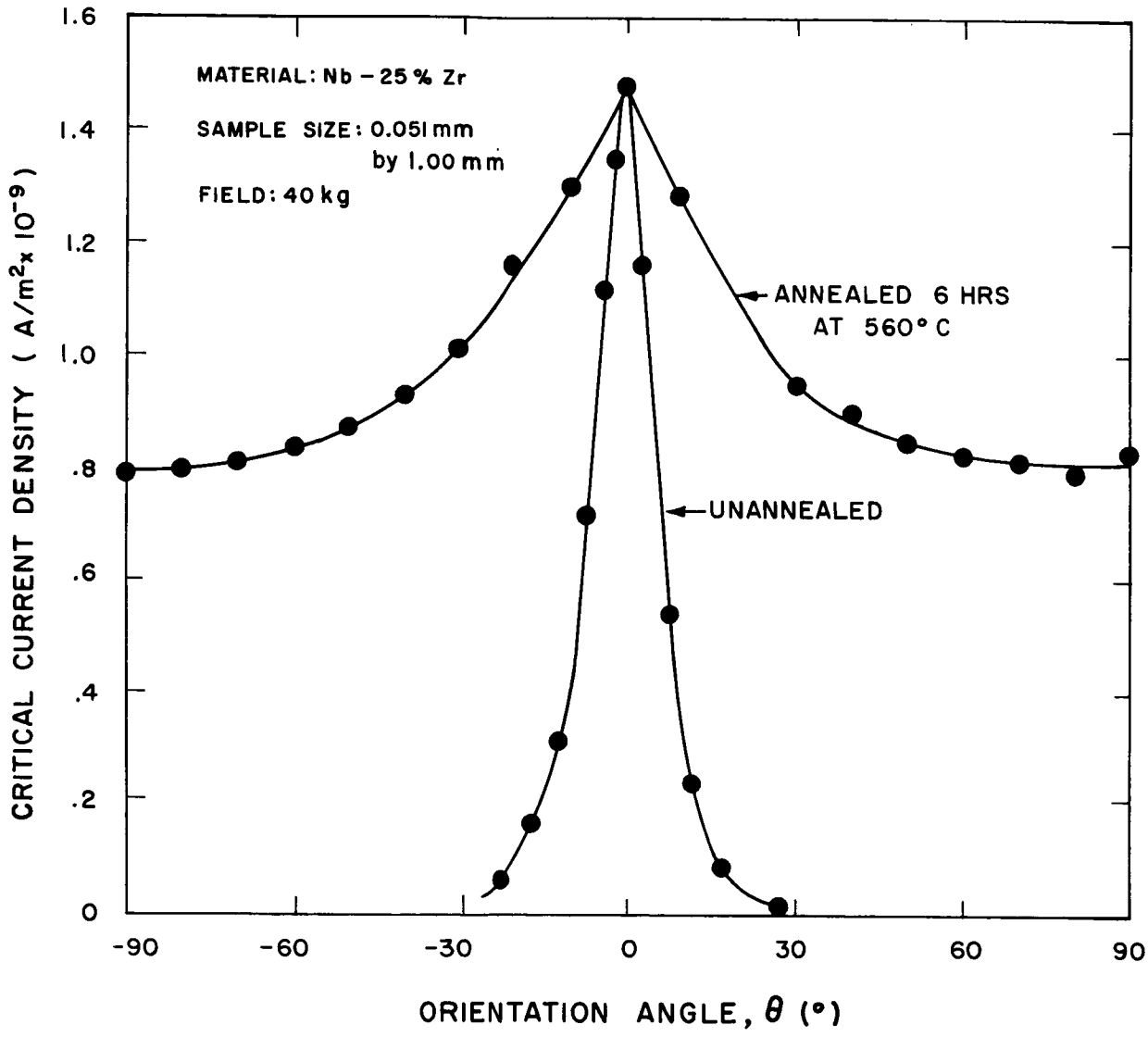

Fig. 5 Typical anisotropy curves for Nb-25% Zr rolled strip 0.051 mm thick by 1 mm wide, showing the effect of annealing.

In order to systematically set forth the results obtained from the various samples we define an anisotropy index, κ, such that

$$\kappa = \frac{\text{current at } \Theta = \pi/2}{\text{current at } \Theta = 0}$$

The possible values of κ can assume a range between zero for highly anisotropic material to unity for isotropic material, e.g., the value of κ for unannealed Nb-25% Zr strip is less than 10^{-2}.

In Fig. 6 the anisotropy index, κ and the critical current density at $\Theta = 0$ and the current density at $\Theta = \pi/2$ in a field of 3.6 T are shown plotted together as a function of annealing time. As seen there the general character of the two curves are the same for each temperature, the only major difference being that the higher temperature curves are displaced toward shorter annealing times.

In each case, κ rises fairly rapidly, then levels off while the maximum critical current density (initially about 18×10^8 A/m^2 for unannealed material) rises slightly, then decreases. An optimum annealing time can be defined for each temperature by taking the time for which the critical current for perpendicular fields is at its peak value.

In Fig. 7, κ is shown plotted as a function of magnetic field. It decreases very rapidly with field, then levels off at a value dependent on the annealing time and temperature.

In order to form a possible explanation for the behavior summarized in Fig. 6 it is useful to observe the phase diagram for the Nb-Zr alloy system as shown in Fig. 8.

Normally in strip manufacture, the alloy is cooled rapidly during the rolling operation from around 1000°C. In such an operation, little or none of the equilibrium phases can precipitate out, so that the end product is a highly cold worked single phase material, full of lattice imperfections aligned in accordance with the rolling plane. These anisotropic lattice imperfections give rise to the extremely anisotropic nature of the material and in general to its high critical current.

Three distinct metallurgical mechanisms exist which, working together, could explain the observed behavior of this material upon annealing. These are:

a) Precipitation of equilibrium phases

b) Coalescence of the grains of precipitate

c) Lattice softening

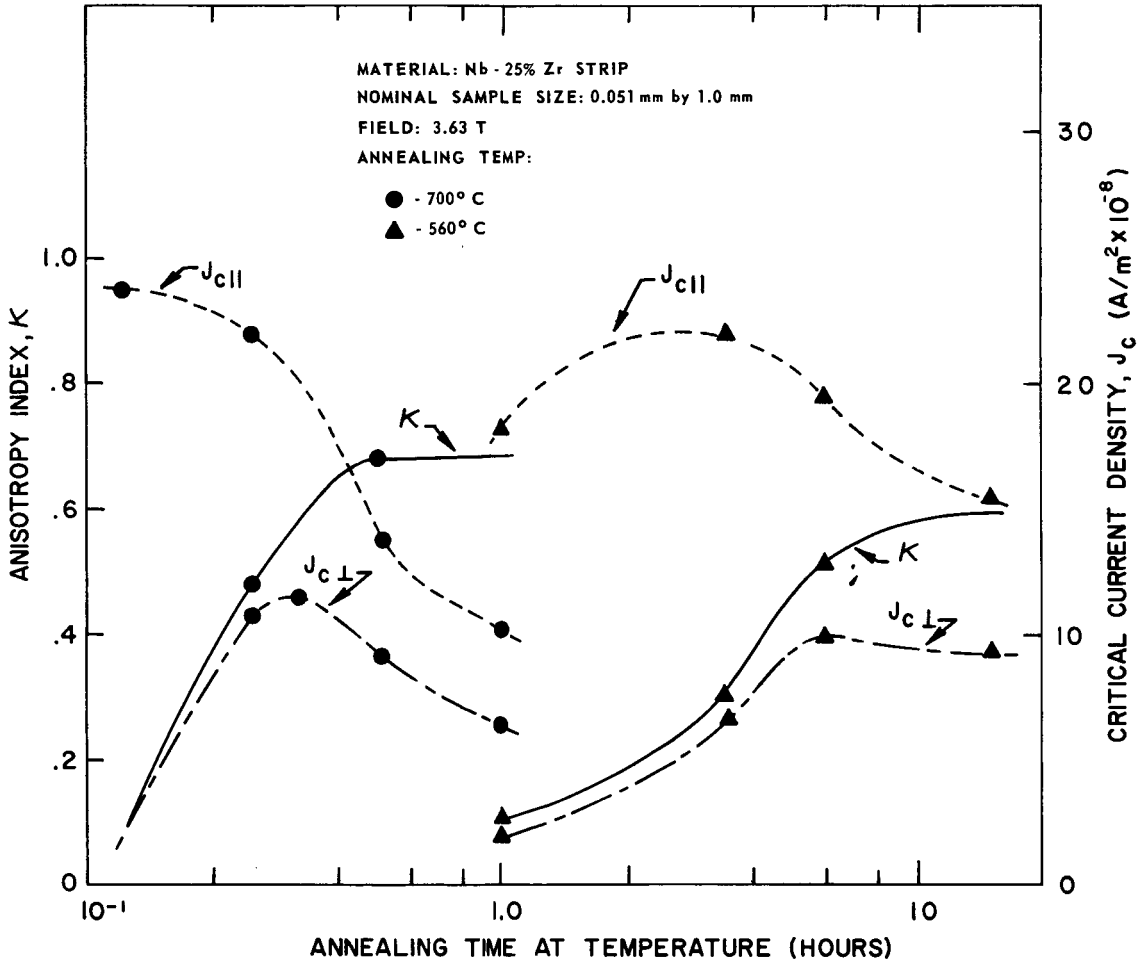

Fig. 6 The effect of annealing temperature and time at temperature, upon the anisotropy index, K and peak critical current density, J_c for Nb-25% Zr strip.

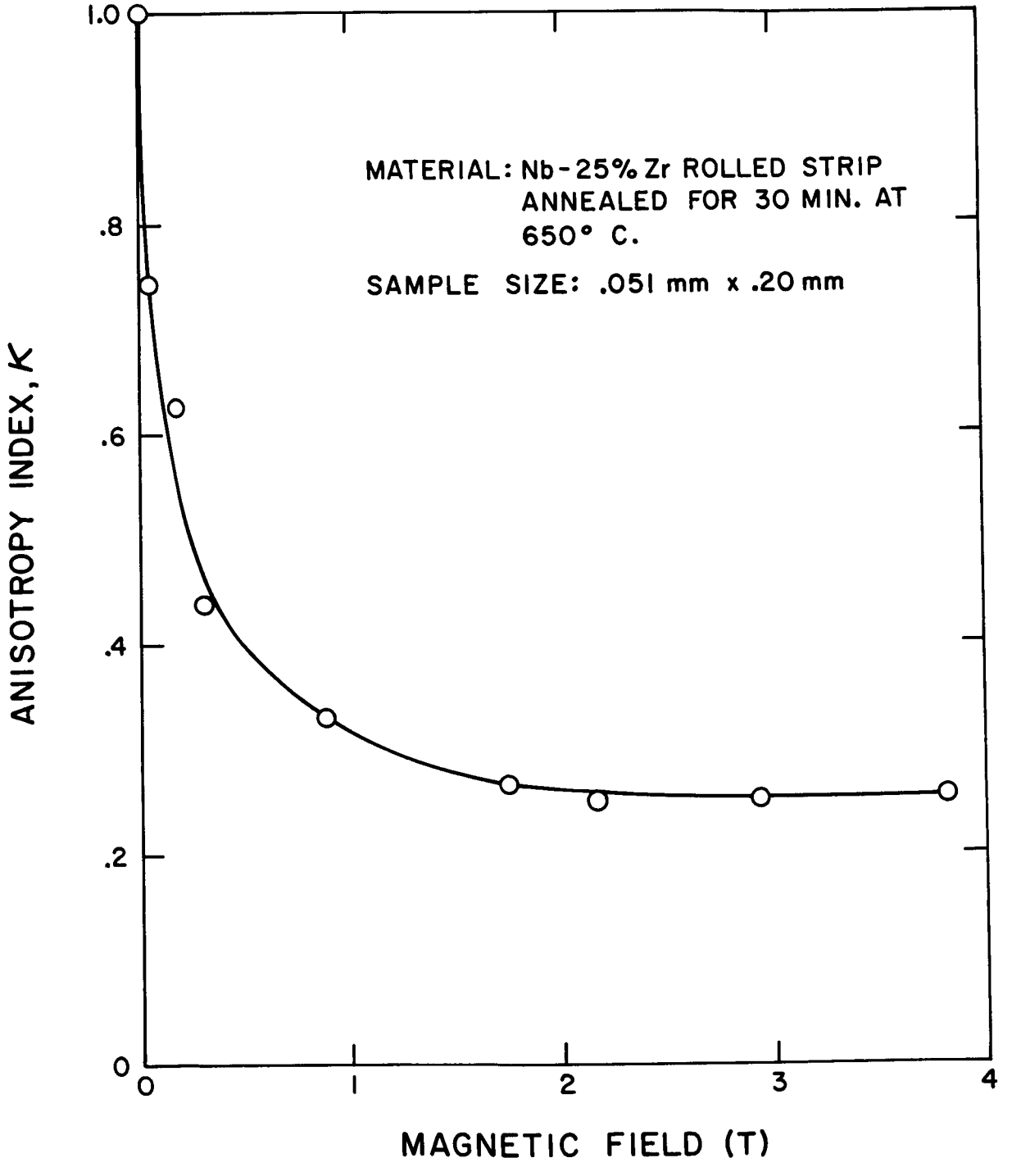

Fig. 7 The effect of magnetic field upon the anisotropy index for annealed Nb-25% Zr strip.

A3307

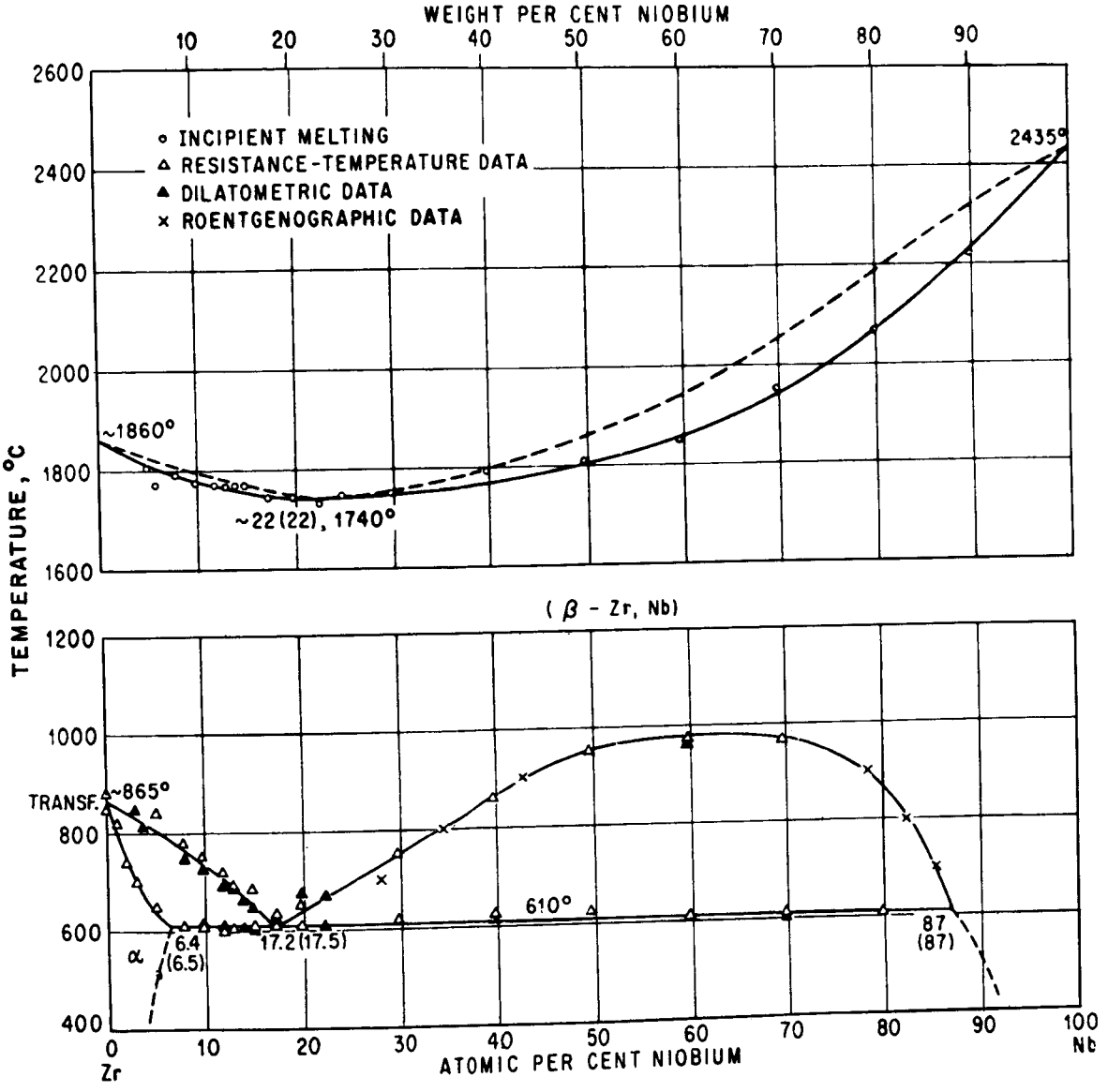

Fig. 8 Nb-Zr equilibrium phase diagram.

During the early stages of the annealing process, small grains of equilibrium phases begin to form, causing lattice strains and in general behaving like lattice imperfections which tend to increase the critical current, thus accounting for the initial rise in critical current. Unlike the imperfections caused by rolling, these are isotropic, hence contribute to the current density at all orientations of the magnetic field, thus accounting for the increase in anisotropy index.

As time goes on, the new grains begin to coalesce. When the number being annihilated exceeds that being nucleated, the total number of new grains begins to decrease, hence the current density begins to decrease. As the available nucleation sites are used up the rate of nucleation diminishes and the anisotropy index begins to level off.

In the final stages of annealing, the lattice is generally softened. This gives rise to a lower normal resistivity and hence lower critical current.

In general, these experiments have shown that it is possible to greatly reduce, though not eliminate, anisotropy by a simple optimum anneal.

IV. TRUNCATION AND ITS REMOVAL BY STABILIZATION

Measurements of the magnetic anisotropy of critical current in samples wide enough for use in large magnets reveal a degradation effect in strip superconductors. This effect (as reported earlier[12, 13]) is manifested as a truncation or "chopping off" of the peaks of the anisotropy curves of these samples. With narrow samples the anisotropy curves (average critical current density plotted as a function of magnetic field direction) normally display a well defined peak centered about the direction parallel to the rolling plane of the strip. With wide samples, however, this peak appears progressively more truncated as the width is increased and the truncation level (i.e., maximum current density) is roughly inversely proportional to the width so that the total current tends to remain constant, independent of width. For Nb-25% Zr strip 0.051 mm thick, this limiting current is approximately 150 A at a field of 4 T for widths between 1 and 10 mm. 1.32 mm wide sample display little or no truncation and have maximum current densities of 18×10^8 A/m^2 whereas 10 mm wide samples show severe truncation and have maximum current densities of 1.5×10^8. This effect has been completely eliminated by stabilizing the strip with copper backing. These results were observed and confirmed in the following experiment.

An annealed sample 3.3 mm wide by 0.051 mm thick (a sample which normally would show severe truncation) was prepared and mounted in the test apparatus as shown in Fig. 9. A 15 cm long section including the necked down test region was stabilized with copper strip. Current from an external supply was fed in by means of this same copper strip and the onset of the normal state was detected by means of a microvoltmeter connected across the test section.

This sample was tested twice, first as described above in its stabilized state and later again with the stabilizing copper separated and electrically insulated from the Nb-Zr just in the test section. The results of these two tests are shown in Fig. 10 where they are compared with earlier results taken on unstabilized samples. The stabilized sample (A31 in Fig. 10) shows complete absence of truncation while in its stabilized state. In its unstabilized state (A31-1) it shows typical severe truncation at a current level equal to that of an earlier completely bare sample (A2) of approximately the same width. Sample A16 is unstabilized but of small enough width so that truncation effects are not noticeable. (The broadening of the peak with sample A31 is due to the heat treatment.)

Similar results were obtained with the same experimental technique on an even wider sample (0.051 mm by 10.5 mm annealed Nb-25 Zr) and these data are shown in Fig. 11. The current density versus angular orientation are virtually identical with those for the 3.3 mm sample.

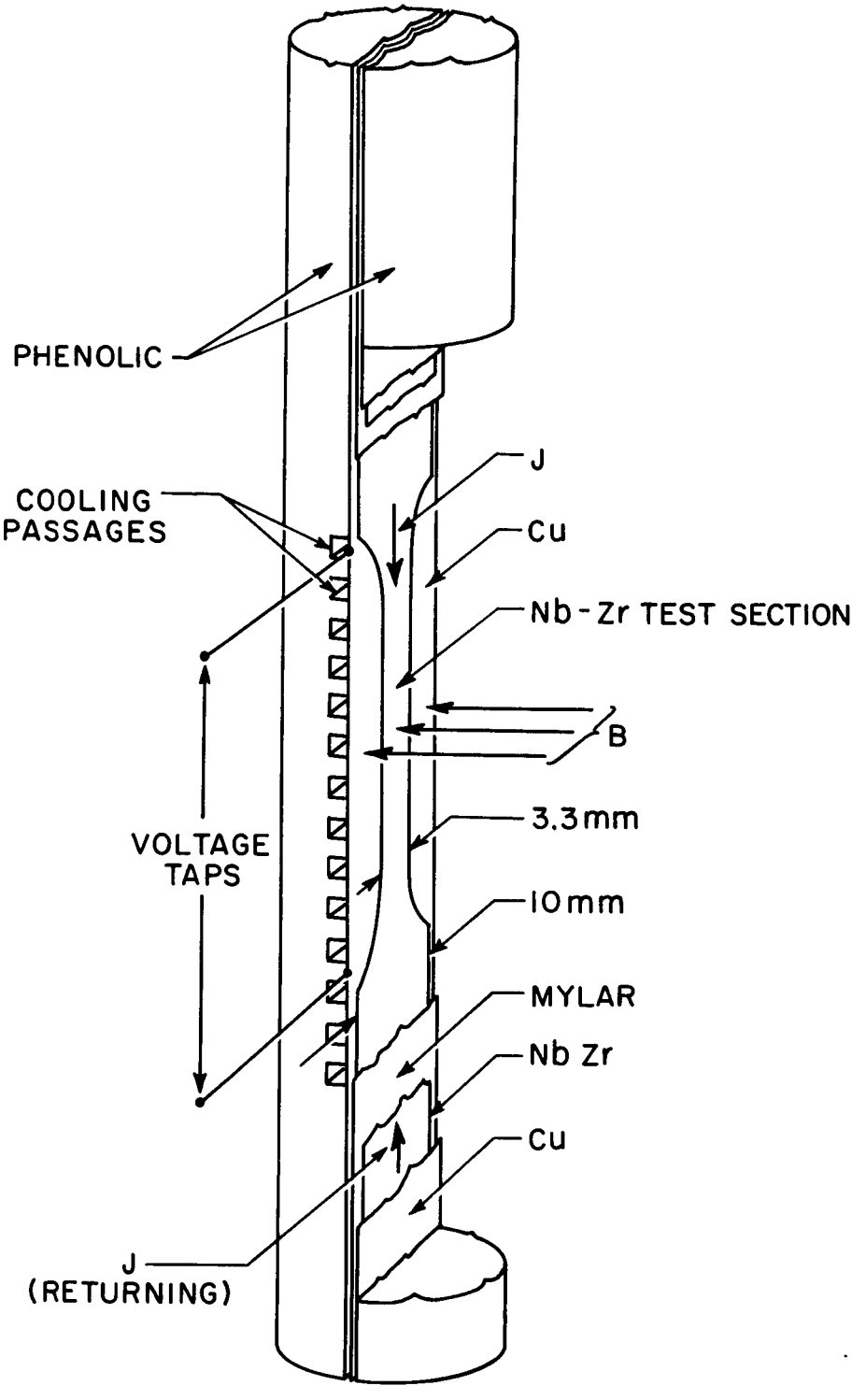

Fig. 9 Stabilized sample mounting arrangement.

A3687

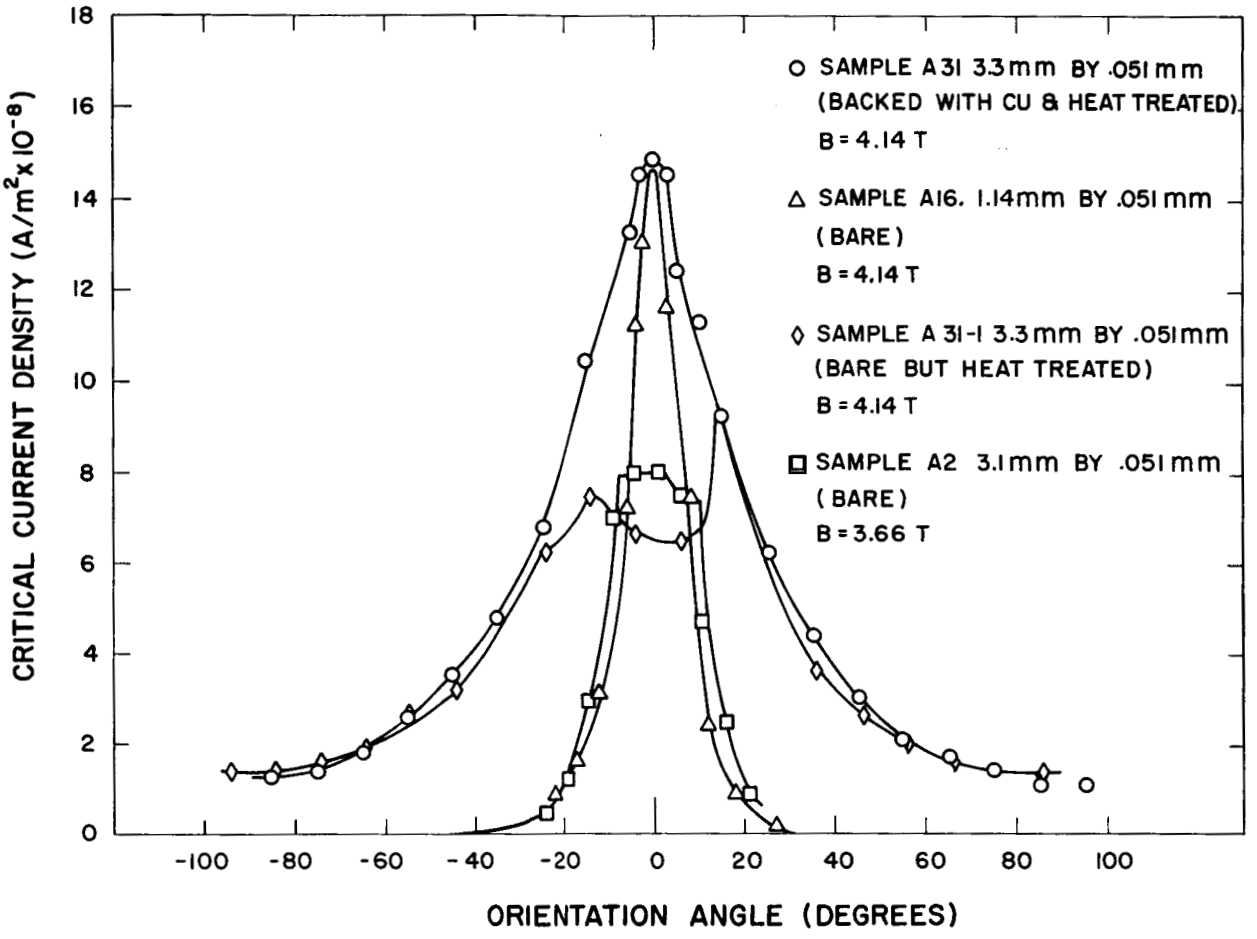

Fig. 10 The effect of stabilization on truncation in a 0.051 mm by 3.3 mm sample of Nb-25% Zr strip.

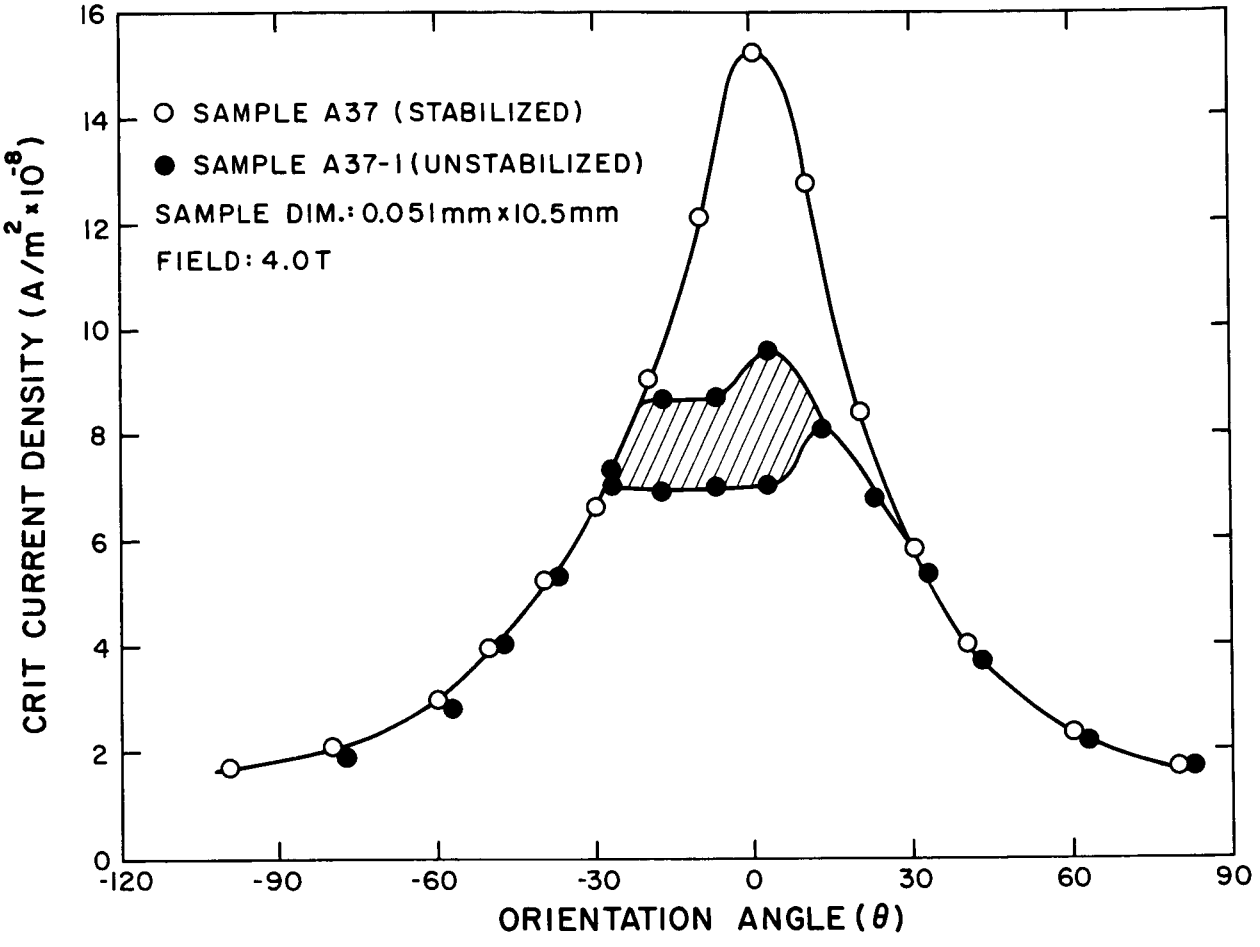

Fig. 11 The effect of stabilization on truncation in a 0.51 mm by 10.5 mm sample of Nb-25% Zr strip. The shaded area indicates the range of data scatter in the truncated region.

A possible explanation of the phenomena of truncation can be developed on the basis of the current density distribution existing on the surface of a strip of infinitely conductive material as predicted from Maxwell's equations. If the actual strip cross section is approximated by an ellipse whose major and minor axes are a and b, respectively, the surface current density distribution can be readily obtained by means of the conformal transformation

$$z = \sin w$$

where z and w are complex variables. (See Appendix A) This was done for the four cases $a/b = 1, \sqrt{10}, 10$ and 100 and the results are shown in Fig. 12. As seen there the maximum surface current density, K always occurs at the extremity of the ellipse where the curvature is maximum. Furthermore, the magnitude of the maximum surface current density, K_m, is proportional to the aspect ratio, a/b, so that

$$K_m = \frac{I}{2\pi b} \tag{8}$$

If it is now assumed that in actual practice the extremities are cooled well enough so that this surface current can in fact penetrate for some distance in from the edge in a more or less stable fashion resulting in a volume current density there instead of a surface current density, then this volume current density, J, flowing inside the cross section would be

$$J = \phi \frac{K}{b} \tag{9}$$

where ϕ is some constant depending on geometry and cooling factors. The parameter ϕ can be looked upon as a ratio Δ/b where Δ is a characteristic distance in from the edge, within which current can penetrate the strip in a stable fashion. In other words, the current tends to flow only in regions of width Δ along each edge of the strip. Using this concept:

$$J_m = \phi K_m/b = (\phi I)/(2\pi b^2) \tag{10}$$

This implies that the total current is independent of width and is of the order

$$I = 2\pi \phi b^2 J_c \tag{11}$$

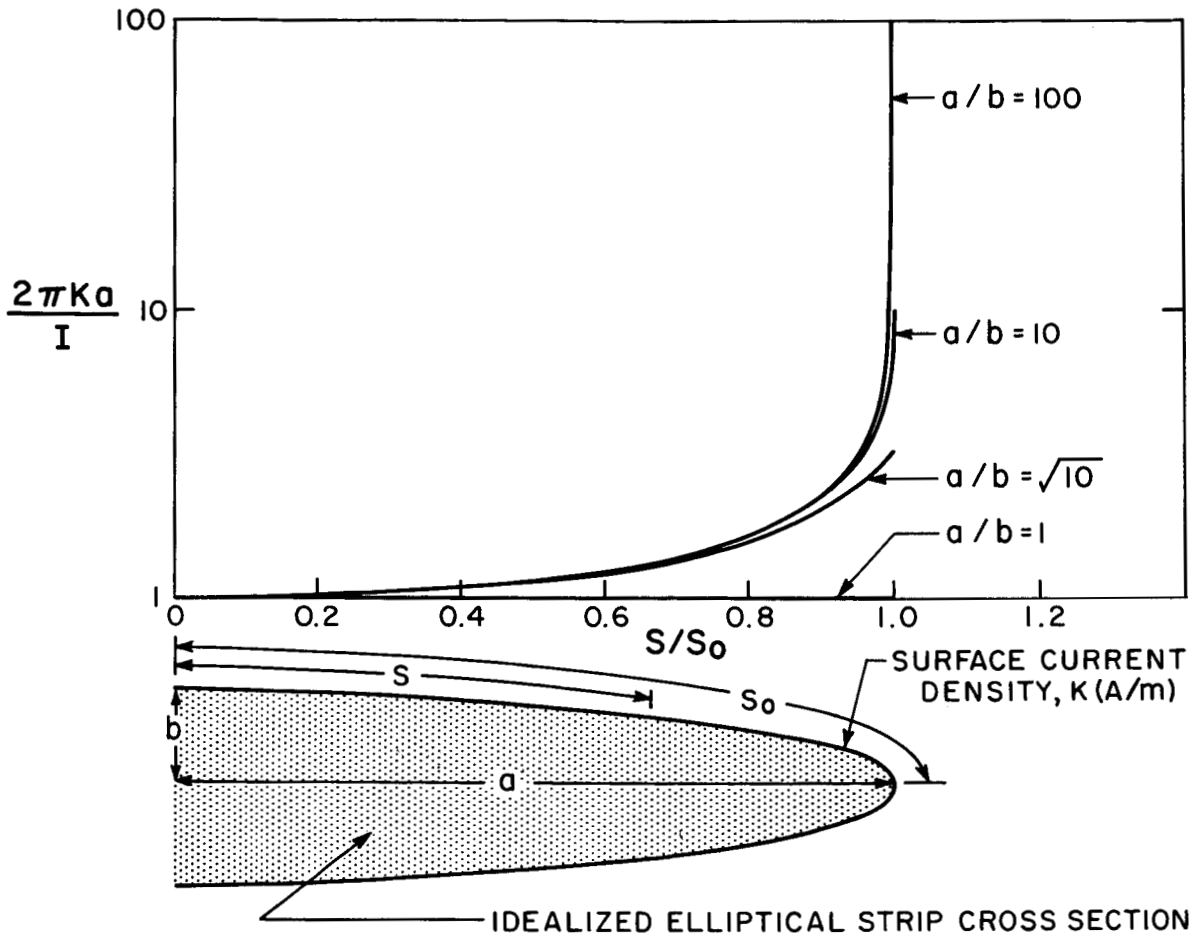

Fig. 12 Surface current density distribution for an infinitely conductive strip of elliptical cross section.

where J_c is the critical current density as given by samples of very small cross section in which truncation is negligible. Typical data from previous measurements on unstabilized strips is given in Table II.[12, 13]

Table II

Total Current vs. Strip Width for Field Parallel to Strip Plane ($\Theta = 0$)

Strip Width (mm)	Total Current (A)
1.32	121
3.07	128
4.80	80
10.0	132

This data shows that the total current does, in fact, tend to be independent of the width. Evidently the center part carries little or no current, hence for strips of width 2Δ or greater the current tends to remain independent of width. If the numbers in Table II are put into Eq. (11) the resulting ϕ is of the order 10, giving a Δ of the order 1 mm. This agrees with the observation that truncation is negligible for strips 1 mm or less in width. The effect of the copper stabilization is to allow the surface current to redistribute uniformly throughout the entire width in a stable fashion instead of just along the edges.

V. PRODUCTION OF STABILIZED STRIP IN LONG LENGTHS

For much of the short sample testing the Nb-Zr strip was stabilized simply by clamping it tightly to the copper during the annealing process. This resulted in a rather weak bond which, though satisfactory for short sample testing, will not withstand the bending and shock of coil winding. Furthermore, this method does not lend itself to the fabrication of lengths suitable for coil winding. Consequently, several methods of laminating long strips were investigated.

The simplest and most effective way found was to plate the strip with copper and then soft solder it to the copper strip. Composite strip made in this way by sandwiching the Nb-Zr between two copper components is very resistant to thermal and mechanical shock and can be bent around a radius of less than 1 cm without damage. This was the material used in the 12.7 cm I. D. solenoid.

Cold rolling and diffusion bonding were also tried as possible laminating methods but neither were found to be satisfactory. The cold rolling failed because in order to obtain sticking of the copper to the Nb-Zr (or even to itself) so much reduction was needed that the resulting elongation fractured the less ductile Nb-Zr component.

In another attempt the Nb-Zr and copper components were first plated with indium and then rolled. It was hoped that indium with its high sticking coefficient would effect a good bond but only minimal success was obtained.

Diffusion bonding was attempted by rolling the composite strip tightly on a spool and heat treating, relying on winding tension to supply the necessary pressure. The bond thus achieved was neither electrically nor mechanically adequate.

For practical coil construction it is essential that some provision be made for making low resistance joints which can be wound into the coil, and that these joints be stable. In addition, it is highly desirable from a fabrication standpoint to devise a method whereby joints can be made after the strip has been laminated with the normal stabilizing metal.

The soldered material lends itself well to the use of lap soldered joints. These joints are made by simply removing the copper from one side of the two ends to be joined and soldering them together as shown in Fig. 13 so that only a thin layer of solder exists between the two superconducting elements. Joints of this type have been constructed with resistances well below 10^{-10} ohms. Although not completely superconducting, such joints

are perfectly adequate for most applications and one has been used successfully in the 12.7 cm I.D. solenoid. With this unit the L/R time constant due to the joint would be in excess of 5×10^7 sec. (> 50 days). If this is not adequate, however, spot welds can be added to make the joint completely superconducting.

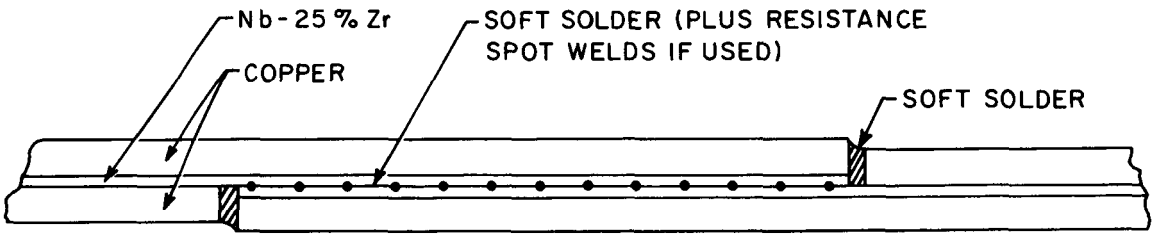

Fig. 13 Typical lap joint between two sections of stabilized superconductor.

VI. A SMALL SUPERCONDUCTING DISK SOLENOID

Before building a strip coil using the stabilization principles outlined above, it was decided to first confirm them on a small coil. To render meaningful results such a coil must have some of the important aspects of the proposed larger coil. It must contain conductors of comparable cross section so that truncation effects, if present, will show up; it must have roughly the same ratio of copper to superconductor and it must be energized with currents at least up to the critical value. For a small coil the associated self fields are small and therefore the currents are apt to be very high, making external energization difficult. Consequently, the only practical way to energize such a coil is by some inductive means.

The superconducting disk solenoid shown in Figs. 14 and 15 meets these requirements quite adequately and was in fact used in an experiment to corroborate many of the predictions of the stabilization theory outlined above. The solenoid consisted of alternately situated copper and Nb-25% Zr disks. The copper disks were 0.51 mm thick and the superconducting disks were 0.051 mm thick. These were optimally heat treated (6 hrs. at 560°C) to reduce anisotropy. The disk dimensions were chosen so that the radial width $(r_o - r_i)$ conformed roughly to the width of the strip to be used in the proposed coil.

The unit was energized inductively by placing it in the field of a one inch I. D. superconducting magnet capable of producing 5 T. Data were taken by means of two bismuth magnetoresistance probes, one on the axis at the center plane and one just outside the solenoid also on the center plane.

The experimental procedure was as follows:

Starting from zero field with the solenoid in the virgin state, the external field was increased positively to 4 T, then back through zero to -4 T, then back through zero to +4 T. Data was recorded by means of an X-Y plotter with the external field on the X axis and the internal field on the Y axis so that with the above energizing sequence a hysteresis loop was traced out. A typical loop for the unit is shown in Fig. 16.

The behavior shown there can be explained in terms of the currents induced in the superconducting disks as the applied field is changed. The change in this applied field as it is increased initially from zero induces currents in the disks of such a magnitude as to create a secondary field equal and opposite to the applied field.

The total effect is therefore to exclude the external field. This exclusion continues to take place as long as the critical current density of the superconducting disks is not exceeded and they do not quench. When the

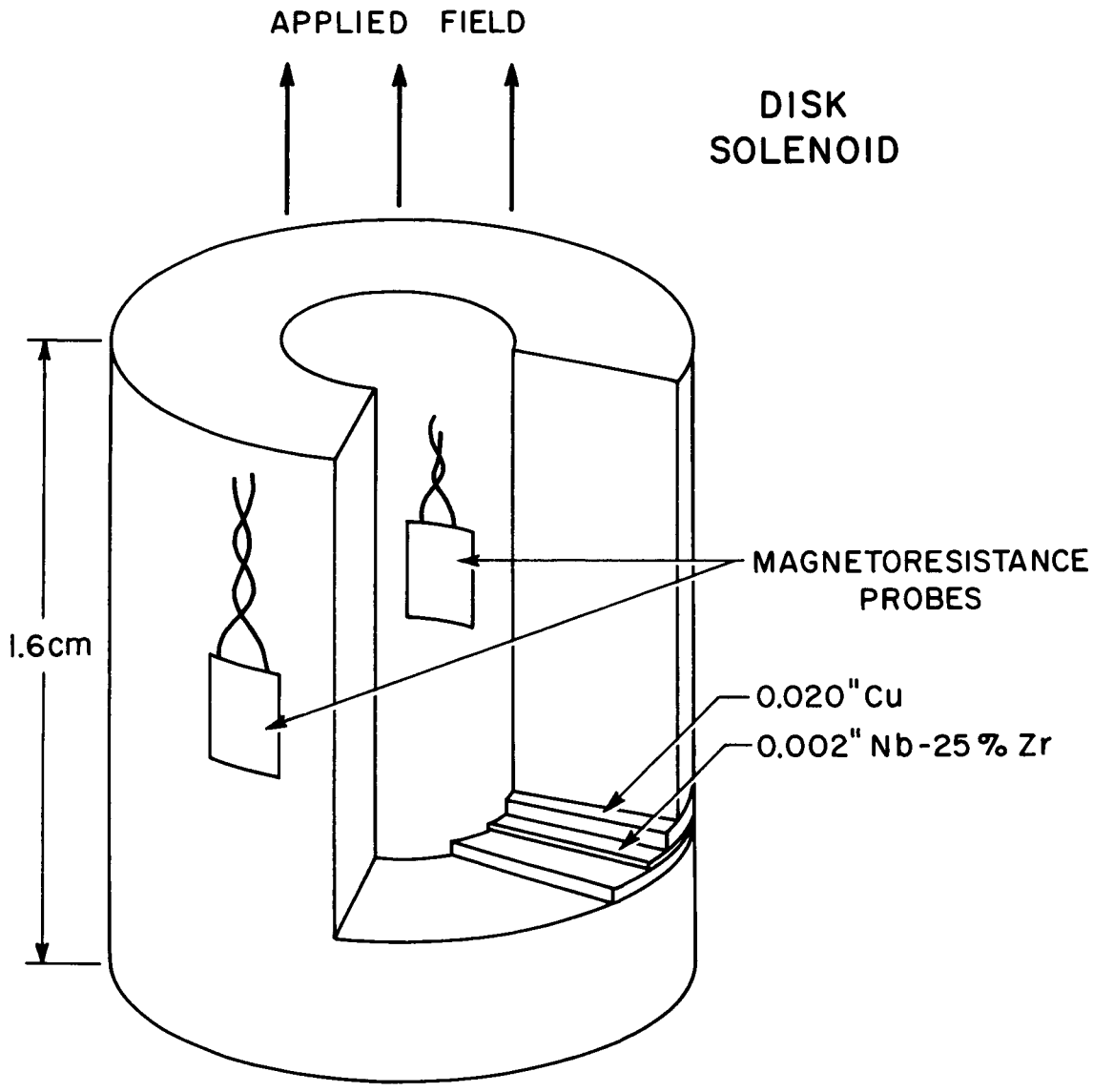

Fig. 14 Schematic illustration of stabilized superconducting disk solenoid showing details of construction and location of magnetic field sensing probes.

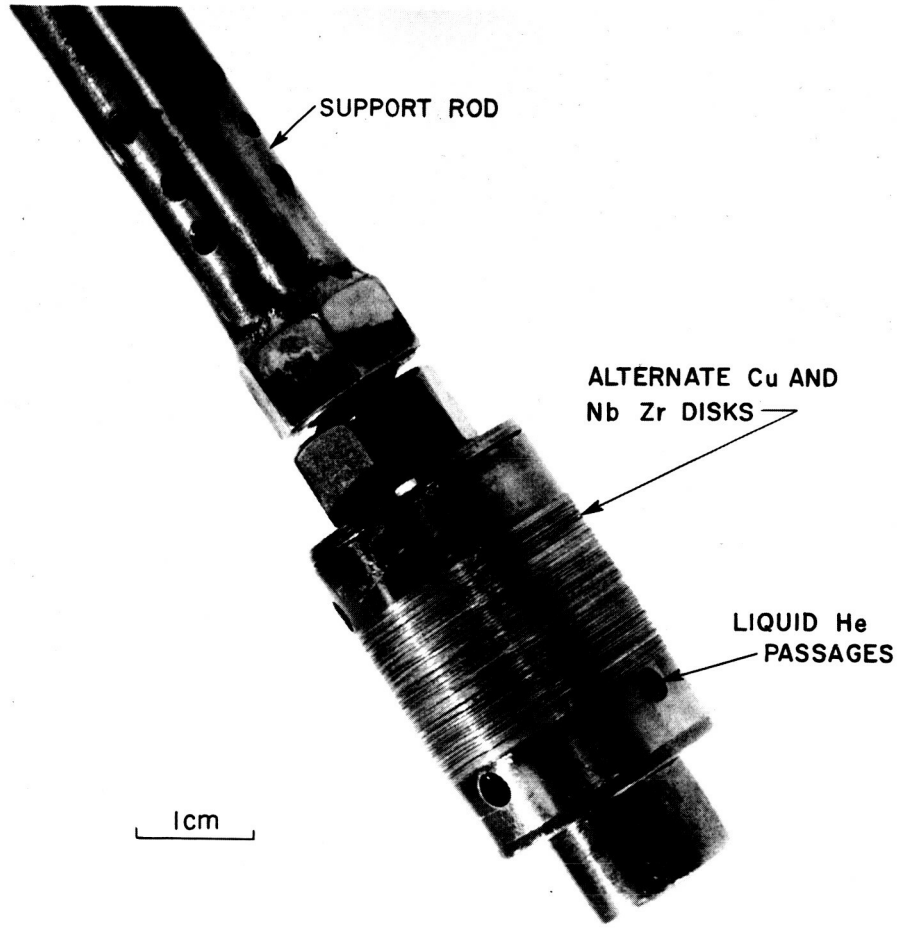

Fig. 15 Stabilized superconducting disk solenoid ready for insertion into helium dewar.

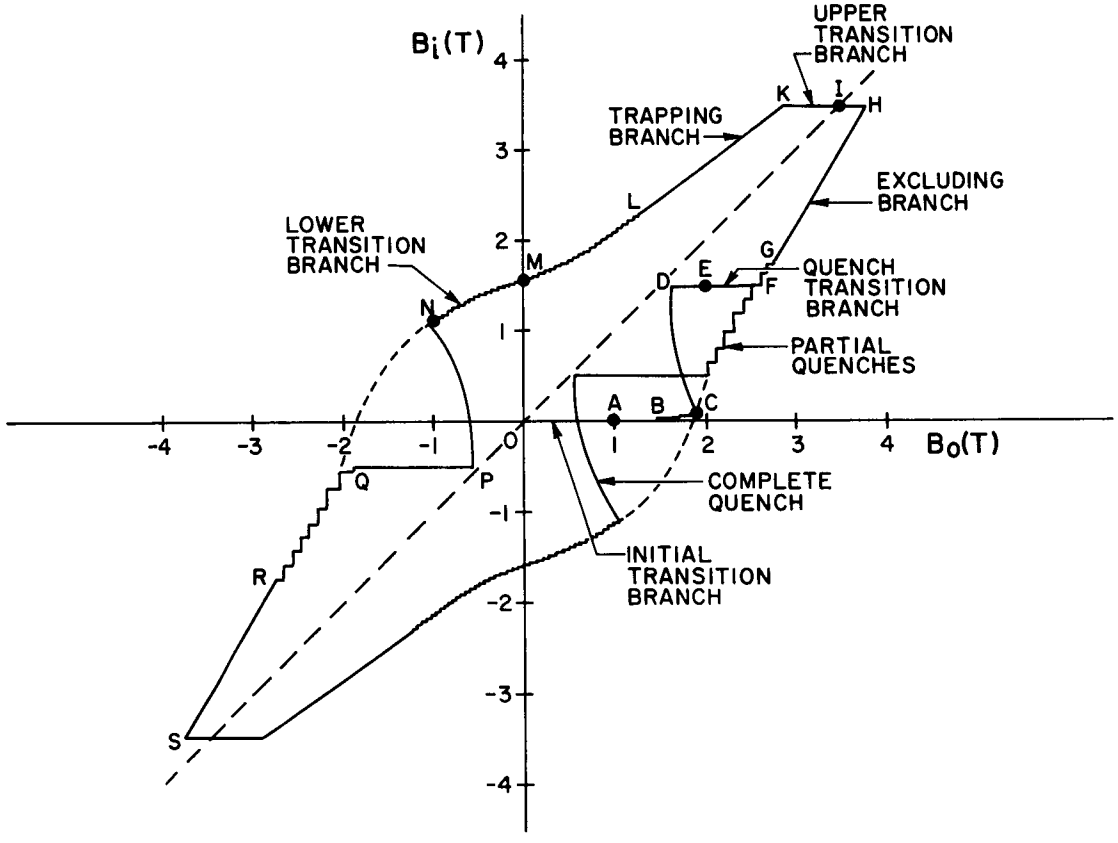

Fig. 16 Typical hysteresis loop for superconducting disk solenoid, showing details of instabilities and quenches.

critical current is exceeded, one of two things can happen. If the solenoid is unstable the joule heating caused by the over-critical current is not carried away effectively and the normal region will propagate causing a partial or possibly a complete quench. If the unit is stable, however, the normal region does not propagate but simply forces the current to redistribute further into the disks. Furthermore, since the inner portions of the solenoid are always shielded from field changes of any sort by induced currents further out, the current density in any completely stable, virgin situation must of necessity be critical or not exist at all. Thus as the applied field is increased initially from zero in a stable situation the field everywhere inside r_i remains zero until the disks are "completely filled" with critical current. Only then does the inside field increase. In a similar manner trapping of the field results as the external field is reduced from a high value to a lower value. These facts were used to calculate the actual current density profile in the disks from the data contained in the stable portions of the hysteresis loop shown in Fig. 16. (Later on the method by which this was done will be described fully but for the moment the results will be used to describe in detail the behavior shown in Fig. 16).

There are several distinct types of branches in the loop shown in Fig. 16. They all relate directly to the flux exclusion and trapping concept described above and are classified as follows:

1) The current transition branch is always characterized by an abrupt change in current density somewhere between r_o and r_i. Typical examples of these branches are o-B, D-F and H-K in Fig. 16. In Fig. 17 the current and field profiles in the solenoid are shown for points A, E, and I respectively which lie within these branches.

2) The excluding branch occurs when the external field is being increased and the current has penetrated the entire solenoid. It is characterized by unidirectional field and current throughout the volume of the solenoid. A typical example is shown in Fig. 18a for point G in Fig. 16 (branch F-H).

3) The trapping branch occurs after completion of the upper transition branch as the applied field is being decreased. Like the excluding branch it is also characterized by unidirectional current and field. A typical example is shown in Fig. 18b for point L in branch K-M.

4) The field transition branch occurs after the trapping branch when the applied field is reduced to zero and then increased in the negative direction. It is characterized by unidirectional current but a field reversal within the solenoid. A typical example is shown in Fig. 18c taken for point N on branch M-N.

The data shown there indicates that the solenoid is stable over most of the field excursion. Only at low field values where the critical currents are high does it become unstable and quench.

The stable portions of the loop in Fig. 16 can be used to calculate the current profiles as follows.

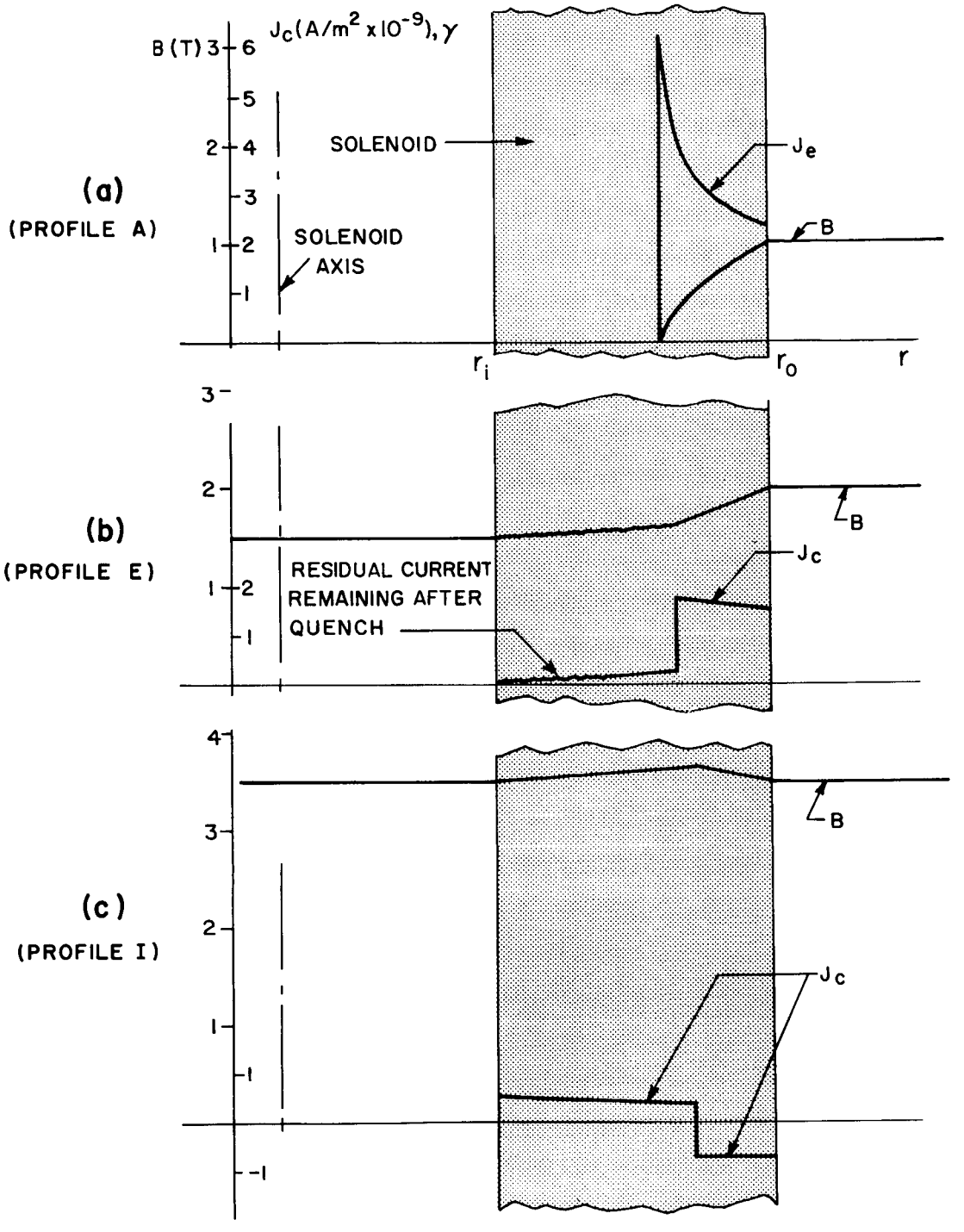

Fig. 17 Current and field profiles for the superconducting disk solenoid taken at three points on the hysteresis loop of Fig. 16.

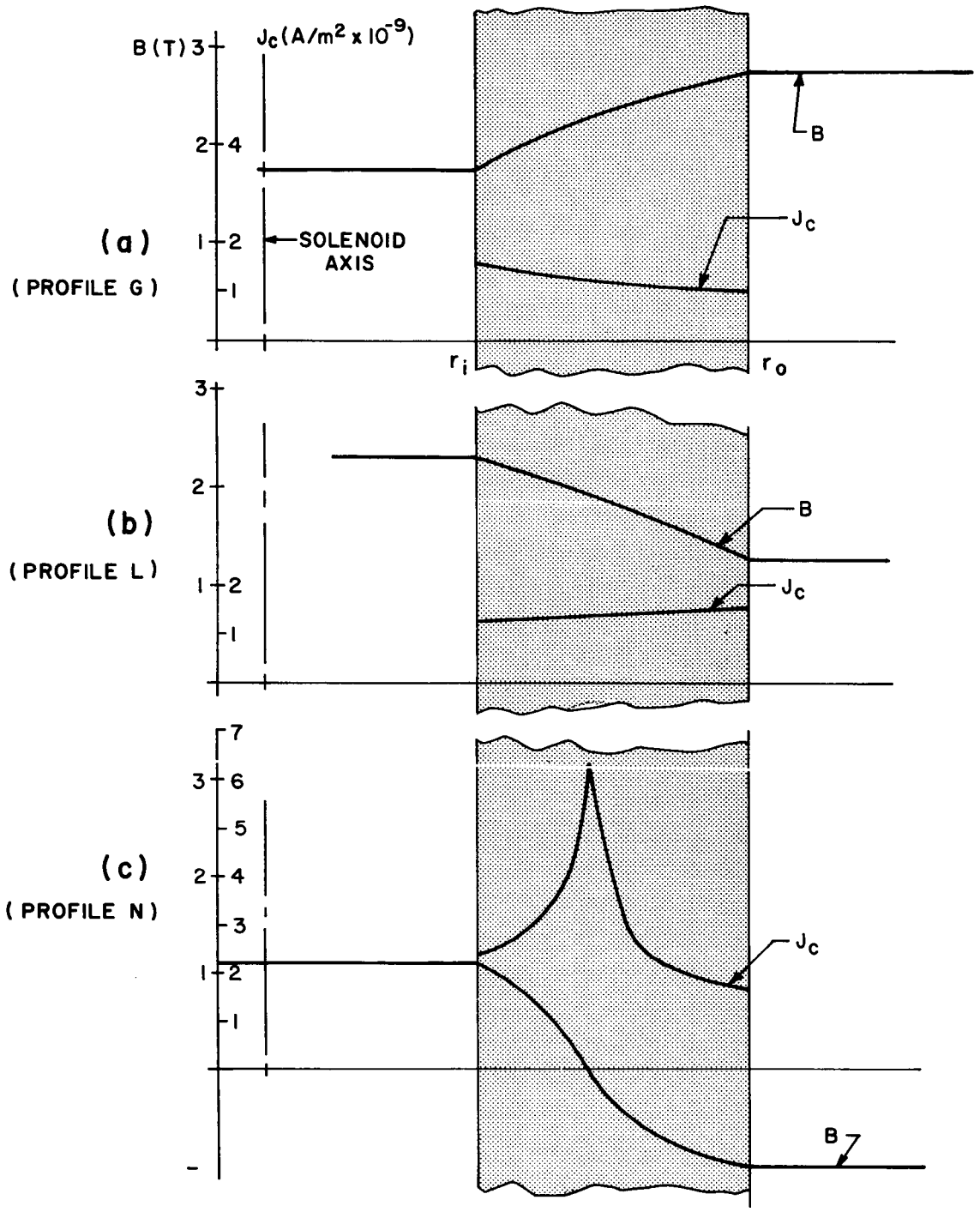

Fig. 18 Current and field profiles for the superconducting disk solenoid taken at three points on the hysteresis loop of Fig. 16.

Assuming that the solenoid is long enough so that the fields observed can be reasonably approximated by those of an infinite solenoid, Ampere's law can be written as:

$$\frac{\partial B}{\partial r} = - \mu_o J. \tag{12}$$

Since $J = J_c(B)$ (i.e., a unique single valued function of the magnetic field) this equation can be written as follows:

$$\frac{dB}{J_c(B)} = - \mu_o \, dr \tag{13}$$

We can define a new variable η such that

$$d\eta = - \frac{dr}{r_o - r_i} \tag{14}$$

and B can now be considered as being a single valued function of η.

Integration then yields:

$$\eta = - \frac{r}{r_o - r_i} + C(B_o) \tag{15}$$

Where $C(B_o)$ depends on the magnetic field at a given point, which is arbitrarily taken to be at the outside radius.

For a given setting of external magnetic field the value of η at the outside radius is:

$$\eta_o = - \frac{r_o}{r_o - r_i} + C(B_o) \tag{16}$$

then at the inside radius:

$$\eta_i = \frac{r_i}{r_o - r_i} + C(B_o) = \eta_o + 1 \tag{17}$$

We are now in a position to calculate B as a function of η, graphically from the data as follows:

1) Using any convenient scale, place a point $[\eta_1 B_{il}]$ as shown in Fig. 19 where B_{il} is the inside field at the top of the trapping branch (K-M) of Fig. 16 and η_1 is any convenient starting point.

2) Place another point $[(\eta_1 - 1), B_{ol}]$ where B_{ol} is the outside field at the same point on the trapping branch of Fig. 16.

3) Sketch in a plausible curve between these two points.

4) Pick a slightly lower value of B_i (i.e., $B_{i2} < B_{il}$) and place it at a point on the sketched curve so that it defines a corresponding new value of η (i.e, $\eta = \eta_2 < \eta_1$).

5) Place a new point $(\eta_2 - 1)$, B_{o2} from the data in Fig. 19 and extend the curve to this new point. By continuing this process along the stable portion of the curve a complete B vs η curve can be obtained. The curve shown in Fig. 19 was in fact obtained from the data of Fig. 16 by working from K to N and then working backwards from S to Q. The two parts were then joined together. In this way the entire curve was obtained in spite of the existence of the quench between N and Q.

From this curve the current density can be obtained from amperes law:

$$J_c = - \frac{1}{\mu_o (r_o - r_i)} \frac{\partial B}{\partial \eta} \qquad (18)$$

This has also been plotted in Fig. 19 along with B. Since the current density J_c shown there is a unique function of B, it can also be plotted directly as a function of B to obtain an H-I curve for the material. This is shown in Fig. 20. It can be shown[14] that for any unique dependence of J_c on B, the hysteresis loop has "folding symmetry" about the 45° line (shown dashed in Fig. 16). However, Fig. 16 does not quite have this symmetry and consequently the current profiles and H-I curves for the trapping branch are slightly different from those for the excluding branch. This is probably due to the fact that the solenoid was not quite long enough to avoid some field curvature near the center plane. With this field curvature a slight error in vertical placement of the magnetoresistance probes (which have an anisotropic field sensitivity) could account for this. This fact is also borne out by the shape of the quench curves in Fig. 16. The curvature from N to P for example is accounted for by the fact that there is some field concentration between the outer edge of the solenoid and the inner diameter of the energizing magnet. When the solenoid quenches this concentration is relieved, thus lowering the external field.

In spite of this asymmetry the two halves agree with each other quite well and are seen also to be similar in character (although somewhat lower)

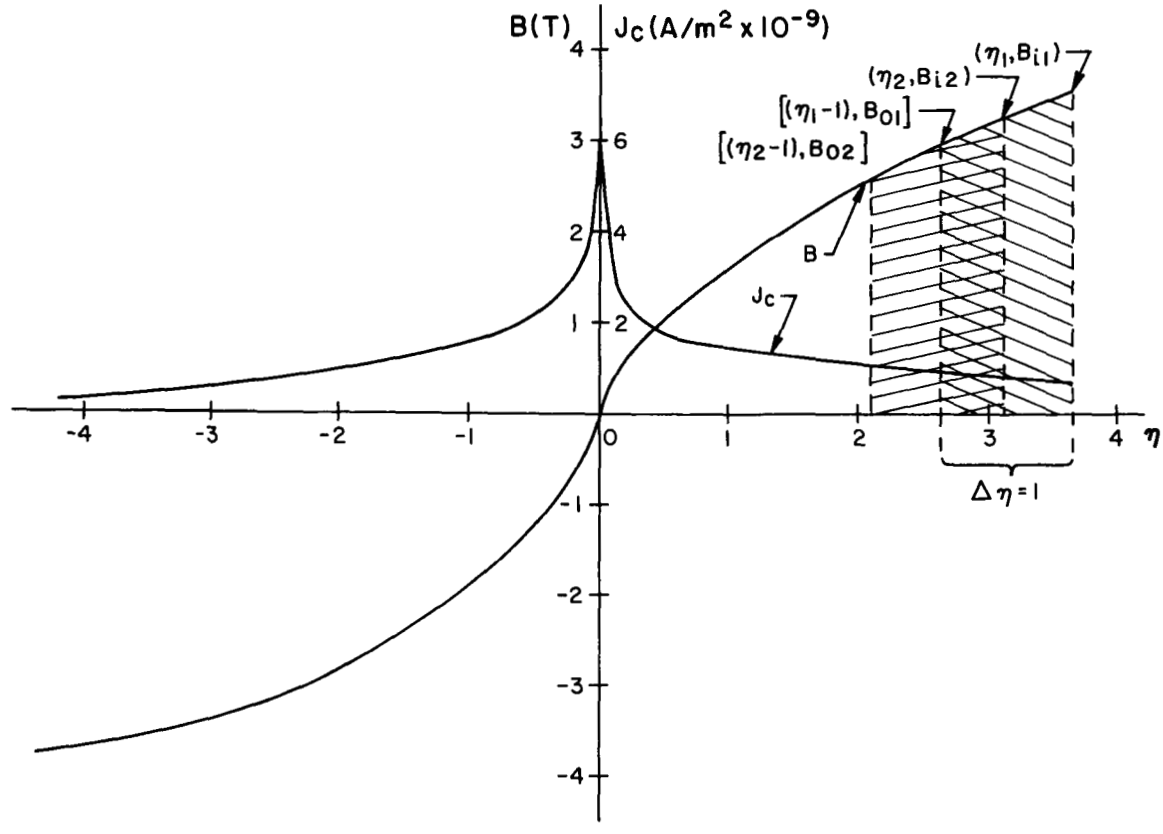

Fig. 19 Current and field plotted as a function of the dimensionless parameter $\eta = r/(r_o - r_i)$ illustrating a graphic method of evaluating the critical current density throughout the solenoid superconducting disk.

to the H-I curves obtained by normal methods for the same material (sample A34 shown also in Fig. 20 for comparison).

The stability of this solenoid cannot be discussed directly in terms of the parameter α derived in Section 2 of this report, since α is field dependent. Since the magnetic field varies considerably from the outside to the inside of the solenoid the question of what value to use arises.

The parameter α as derived in Section 2 is the ratio of the temperature that would result if all the current flowed through the substrate alone to the critical temperature of the superconductor in the presence of the original magnetic field, but with no current in it.

Let us first derive an expression for the temperature that would exist with all the current flowing in the normal substrate. We shall do this for the geometry shown in Fig. 21, and assume that it is part of an infinite solenoid so that we will neglect end effects. The characteristic time $\tau = (\pi r_o^2 \mu_o)/(2\rho)$ for current to redistribute is of the order of 1 sec for this device. Since this time is long compared to the transients normally associated with instabilities of this type we assume that the current distribution in the copper is the same as it was in the superconductor.

If the disk is assumed to be part of an infinitely long solenoid, then the difference between internal and external magnetic field is

$$\Delta B = \mu_o \int_{r_i}^{r_o} J_c \, dr \tag{19}$$

The heating in a length δ, assuming a copper resistivity of ρ is

$$q = 2\pi\rho\delta \int_{r_i}^{r_o} J_c^2 \, r \, dr \tag{20}$$

This can be normalized to the average current density

$$J_{av} = \frac{\int_{r_i}^{r_o} J_c \, dr}{r_o - r_i} = \frac{\Delta B}{(r_o - r_i)\mu_o} \tag{21}$$

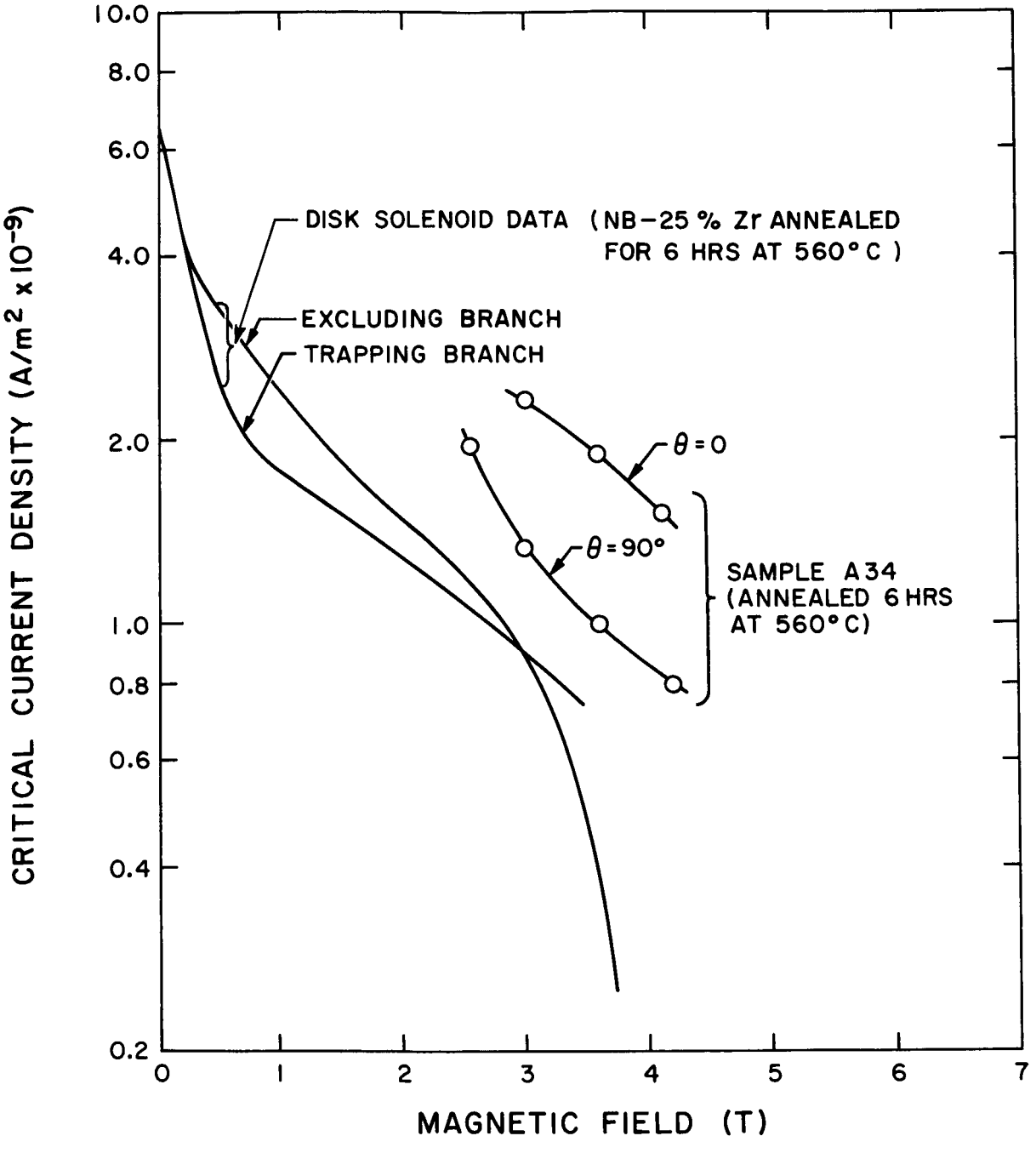

Fig. 20 H-I curves taken from data contained in the exclusion and trapping branches of the disk solenoid hysteresis loop. Short sample data for similar strip material are also included for comparison.

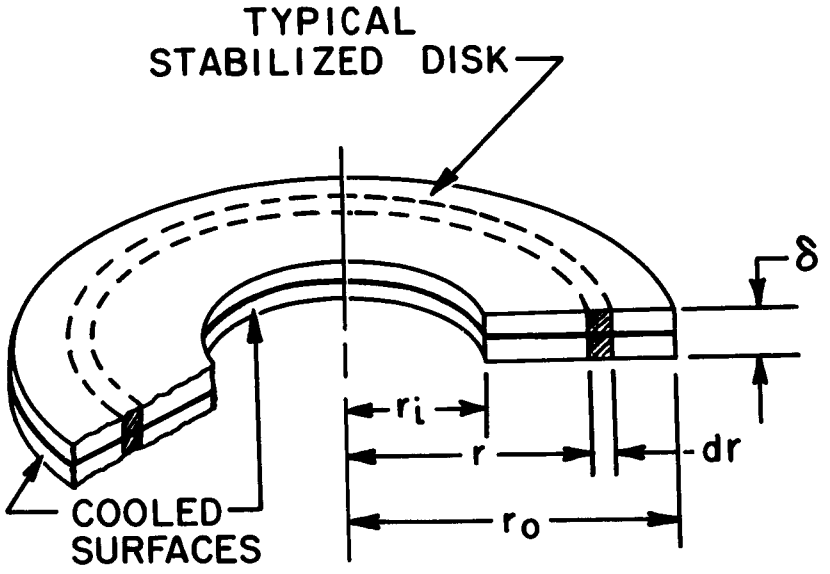

Fig. 21 Schematic illustration of a single stabilized disk of the solenoid, showing method of deriving the local stability parameter.

so that

$$q = \frac{2\pi\rho\delta(\Delta B)^2}{\mu_o^2 (r_o - r_i)^2} \int_{r_i}^{r_o} \left(\frac{J_c}{J_{av}}\right)^2 r\,dr \tag{22}$$

The temperature rise is

$$\Delta T = \frac{q}{2\pi h\delta (r_o + r_i)} \tag{23}$$

Substitution then results in

$$\Delta T = \frac{\rho (\Delta B)^2 \int_{r_i}^{r_o} \left(\frac{J_c}{J_{ave}}\right)^2 r\,dr}{\mu_o^2 h (r_o - r_i)^2 (r_o + r_i)} \tag{24}$$

This is the temperature which would exist if all the current flowed in the normally conducting material. If at this temperature the superconductor is anywhere within the coil below its critical temperature, then it will locally begin to short out the normal substrate and all the current will transfer to the superconductor. It should be emphasized that the superconductor need be superconducting only at the lowest value of magnetic field, since if it takes on current at this point, this decreases the current in the substrate, and the heating decreases allowing further transfer of current to the superconductor.

The stability parameter can therefore be defined as:

$$\alpha_{eff} = \frac{\rho\Delta B^2 \int_{r_i}^{r_o} \left(\frac{J_c}{J_{ave}}\right)^2 r\,dr}{\mu_o^2 h (r_o + r_i)(r_o - r_i)^2 (T_{ch_{max}} - T_b)} \tag{25}$$

where $T_{ch_{max}}$ is the maximum critical temperature which exists in the solenoid at any time.

The demarcation between stable and unstable operation is as before $\alpha_{eff} = 1.0$ with stable operation occurring for $\alpha_{eff} < 1.0$.

The stability is seen to depend on the amount of magnetic field trapped or excluded as well as the maximum critical temperature. The maximum value of ΔB occurs in the second and fourth quadrants in Fig. 16 and it is in these quadrants that the quenches occur, showing that almost complete stability has been achieved.

So far it has been tacitly assumed that the heat capacity is very small and the heat transfer very high in the copper so that there are essentially no temperature gradients. However, the presence of minor instabilities (C-F, L-N, etc. in Fig. 16) suggests that there may be some temperature gradient effects. The instabilities between C and F and between Q and R for example are much larger than those between L and N. In the excluding branch the highest current density occurs at the inner radius where the cooling area is small and obstructed, whereas with the trapping branch the reverse is true. The existance of temperature gradients could account for this difference in flux jump size by causing greater temperature rises at the inside than at the outside for a given amount of current transfer.

In order to strengthen this conjecture the solenoid was wrapped with mylar tape to reduce the heat transfer to the helium. The results of this experiment are shown in Fig. 22. As seen there the operation is extremely unstable showing that heat transfer is in fact an important consideration. Here as in Fig. 16 the trapping instabilities are smaller than the excluding instabilities.

The surface contact between the copper disks and superconducting disks also has some effect on the operation of the solenoid. The experiments just described were done with the superconducting disks bare. A second experiment was done with copper plated disks (with the same optimum anneal). The data for this unit is shown in Fig. 23. In can be seen there that the unit is somewhat more stable as evidenced by the absence of the small instabilities in the trapping branch and the reduced size of the instabilities in the excluding branch. In fact on one occasion starting with the virgin state the complete exclusion branch was traced without any complete quenches. This was never achieved with the unplated unit. Evidently the instabilities of the unplated unit resulted in a lower apparent current density because the H-I curve taken from the plated unit (see Fig. 24) is somewhat higher and in fact correlates almost exactly with short sample data.

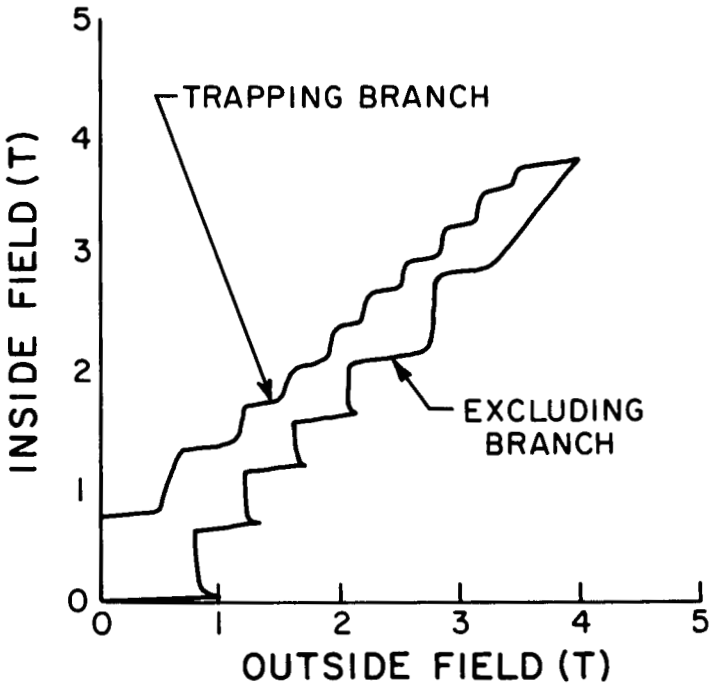

Fig. 22 Trapping and exclusion loop for poorly cooled solenoid, showing extreme character of instabilities.

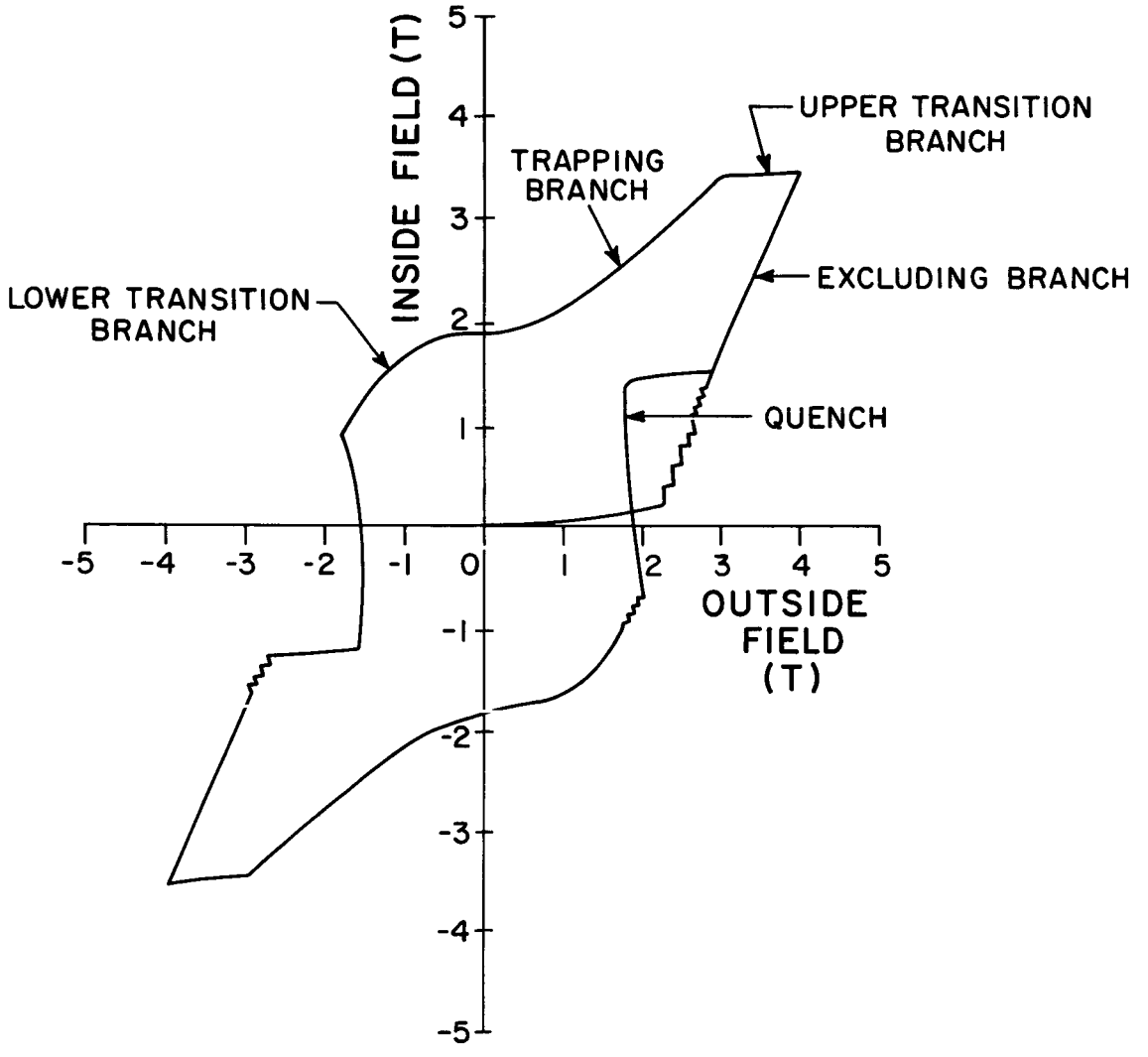

Fig. 23 Typical hysteresis loop for superconducting disk solenoid with copper plated disks.

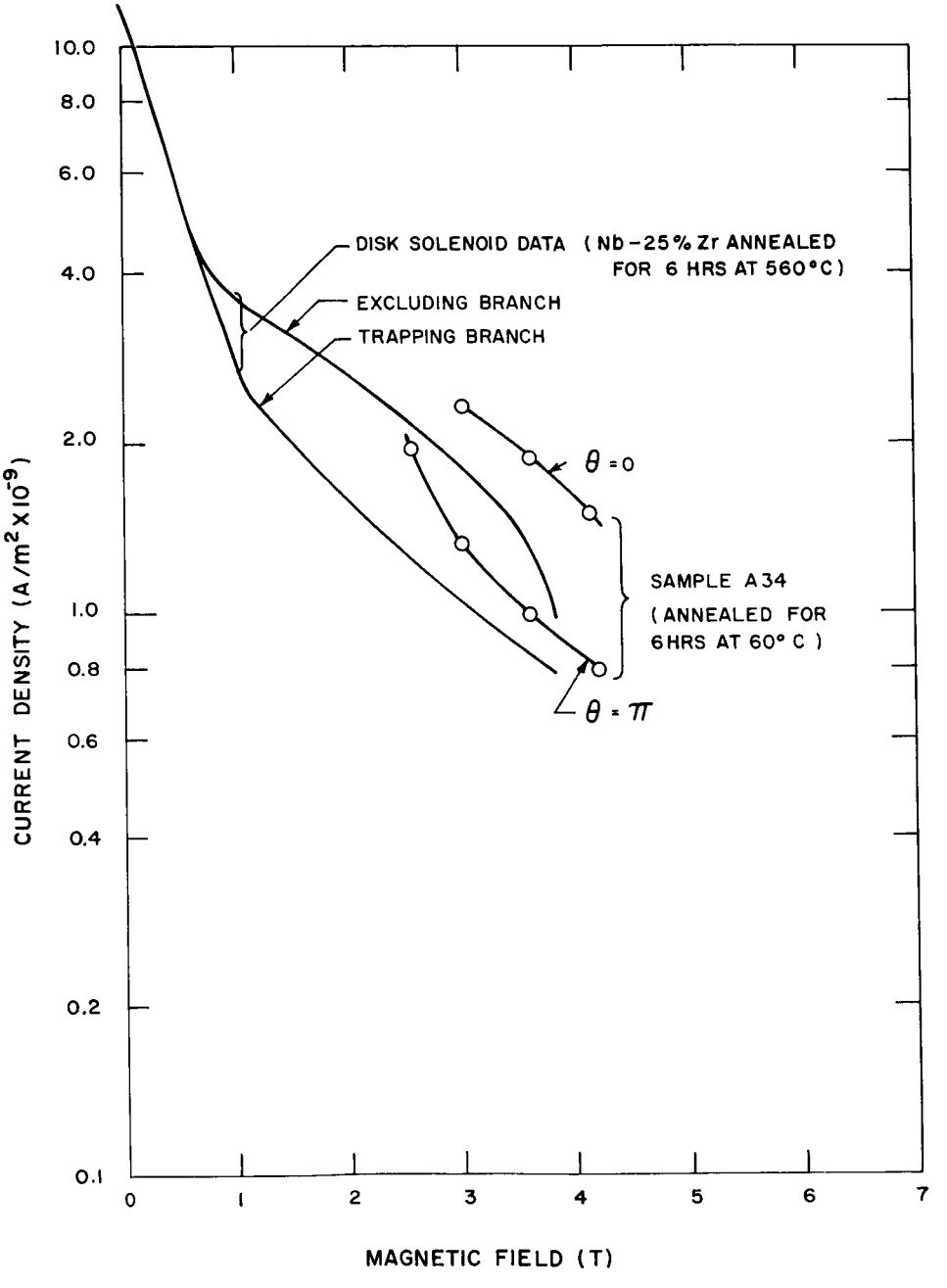

Fig. 24 H-I curves taken from data contained in the exclusion and trapping branches of the disk solenoid with copper plated disks. Short sample data for similar material is also included for comparison.

VII. THE 5-INCH ID NB-ZR STRIP COIL

Using only short sample data obtained in the experiment described above, a 12.7 cm (5 in.) I.D. 25.4 cm (10 in.) O.D. solenoid was designed and constructed. The unit consisted of a single module comprising two series pancake type coils phased so that the cross connection between the two occurred at the inner diameter. The conductor consisted of copper plated, optimally annealed Nb-25% Zr strip 0.051 mm (0.002") thick by 1.27 cm (0.5") wide soldered between two copper strips, each 0.38 mm (0.015") by 1.27 cm (0.5") wide.

Heaters and carbon resistance thermometers were placed near the inner radii and at other strategic locations and a total of 52 voltage taps were brought out for observing normal regions created by these heaters.

The unit is shown in Fig. 25 ready for insertion into the test dewar. Its specifications are given in Table III.

Table III

I.D.	12.7 cm (5")
O.D.	25.4 cm (10")
Length	3.5 cm (1.38")
Coils per module	2
Turns per coil	43
Total inductance of module	5 mH
Field-current ratio	5.8×10^{-4} T/A
Minimum predicted center field	1.1 T
Minimum predicted current	1850 A
Actual center field	>1.2 T
Actual current	> 1900 A
Actual overall current density	$> 1.16\ 10^8$ A/m^2
Actual current density in superconductor	$28.6\ 10^8$ A/m^2
Mass of superconductor in module	0.27 kg
Mass of copper in module	4.39 kg
Dimension of Superconductor	0.051 mm by 1.27 cm (0.002" by 0.5")

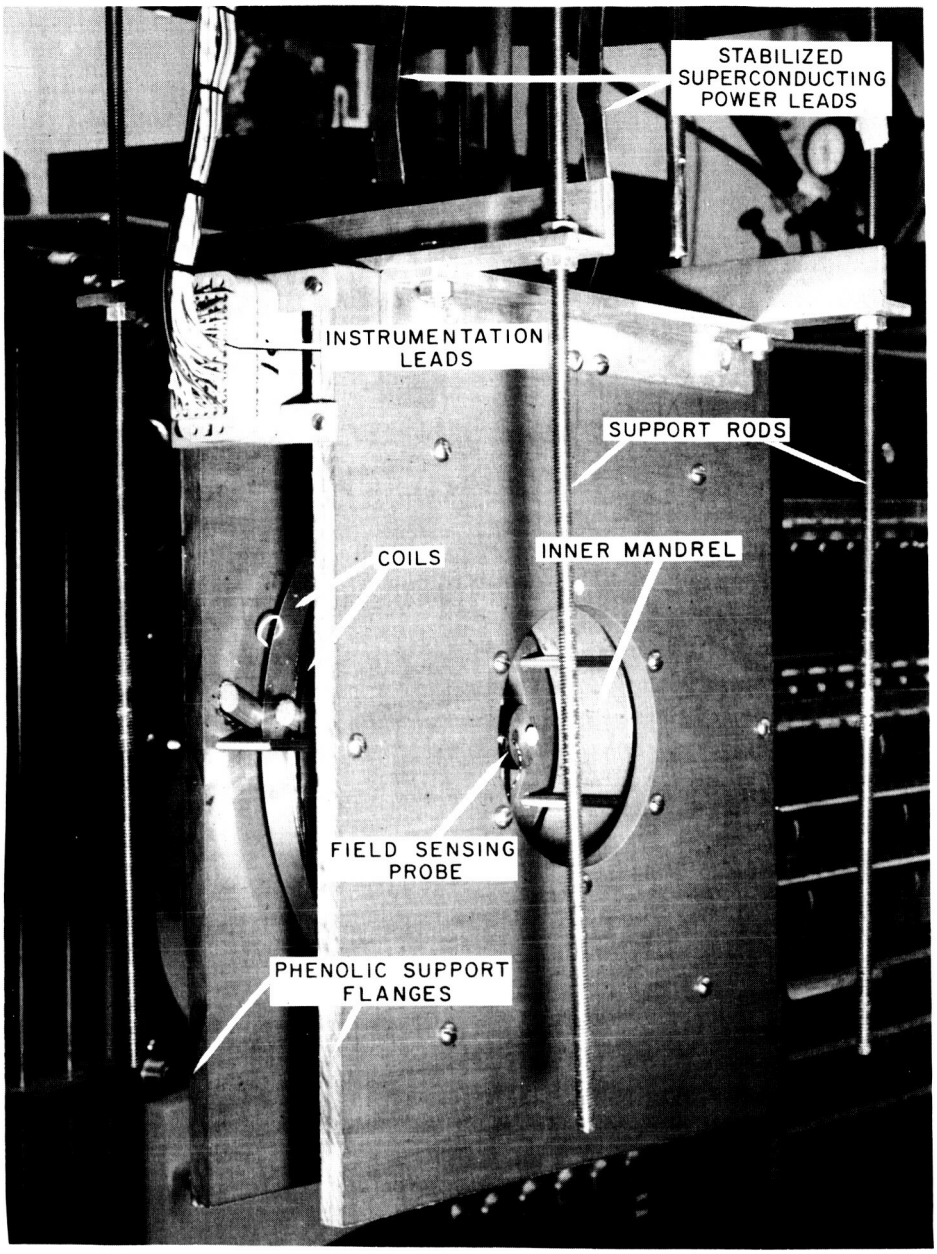

Fig. 25 The 12.7 cm I. D. stabilized superconducting strip magnet shown ready for insertion into the test dewar.

A3843

Two types of joints were used in the coil, spot welded joints between Nb-Zr strips before lamination and solder joints between sections of the component strip after lamination. There were several of the former and one of the latter in the coil. No measurable voltage could be detected across either type during operation even at the highest currents.

The coil was energized by means of a 4 V, 2000 A, D. C. supply connected to the coil by means of leads cooled by the helium boil-off gas from the dewar. The terminals at the top of these leads were cooled by liquid nitrogen. This arrangement increased the peak current capability of the helium cooled leads and lowered the heat leak between tests.

The coil performance was better than the minimum predicted performance given above in Table III and it could not be driven normal with the current supply available. The correlation between actual and predicted performance is illustrated in Fig. 26 which shows the current, field characteristics of the coil plotted along with the H-I curve for the superconductor with which it was wound. The intersection of the two curves gives the predicted performance. Two sources of H-I data are shown in Fig. 26, a short sample (Sample A34) tested in the conventional way and data obtained from the disk solenoid. In order to take into account the anistropy effects of the strip the H-I curves for both the parallel and perpendicular cases are given for the short sample. The perpendicular case gives the minimum predicted performance. The data from the disk solenoid is included as a check, and lies between the other two curves. (This is to be expected since the data is an average of the whole range of orientations in the disk solenoid). As seen in Fig. 26 the actual performance lies above the minimum predicted by the intersection.

Tests also indicated that the coil was predictably influenced by the heaters. These tests involved the use of a heater in the form of a thin strip of nichrome wound in close thermal contact (though electrically insulated) with the conductor near the inner radius so that a single complete turn could be heated. Seven voltage taps were spaced at equal intervals around this turn so that the voltage per unit length could be obtained for any desired portion of this heated turn. The test procedure involved setting the coil current at various fixed values and then varying the heater power. Data was obtained by recording simultaneously the voltages across twenty-six sections of the coil (including the seven sections in the heated turn), plus the heater current, the heater voltage and the coil current, all as a function of time. In addition, the voltage across the center section of the heated turn was plotted as a function of heater current by means of an X-Y recorder connected in parallel with the multi-channel time base recorder. The resulting data was in the form of a series of curves of conductor voltage drop versus heater current at various fixed coil currents.

The data can be interpreted in terms of the theory derived in Section 2 of this report.

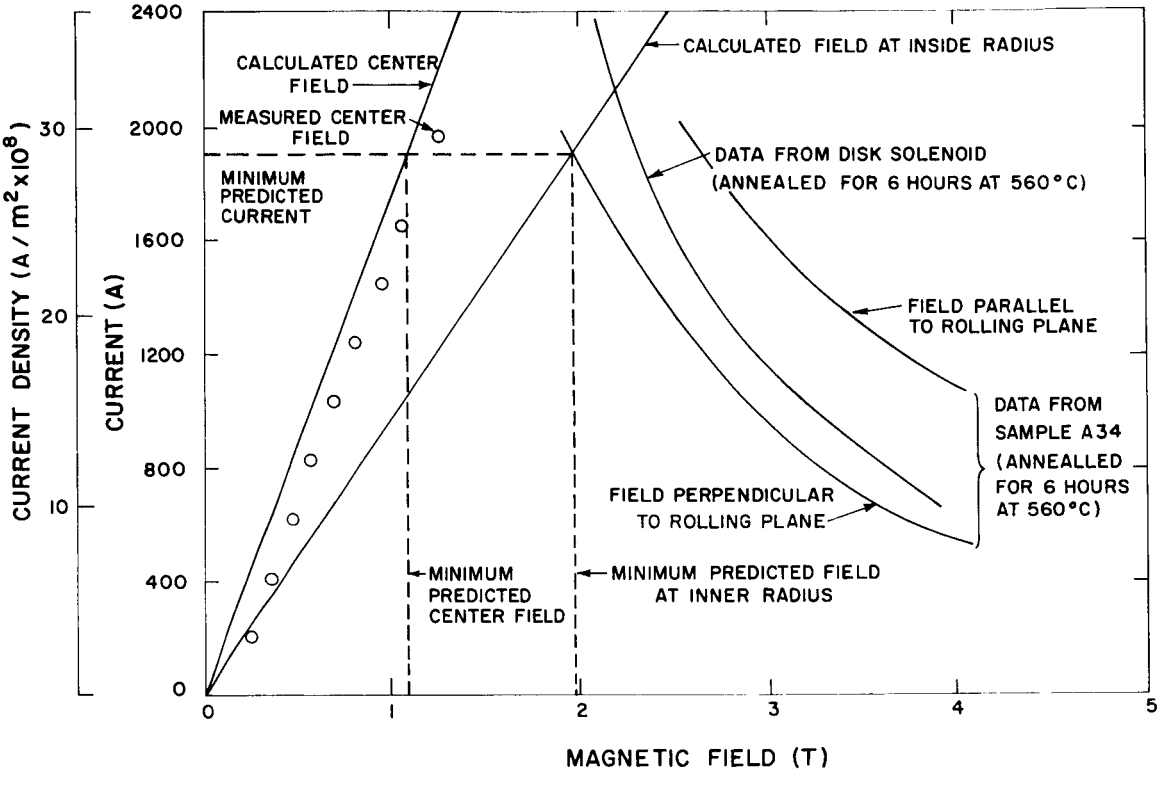

Fig. 26 Design curves for the 12.7 cm I. D. stabilized superconducting strip magnet, showing predicted and realized performance.

Figure 27 shows the heat required for a voltage to appear in the heated section of the coil. Extrapolation of the data to zero heat input should yield the critical coil current at the heated section. Since the heated section is in the third turn (out of 43 turns) from the inside of the coil the actual critical current of the coil should be less than the extrapolated value.

Figure 28 shows the data for voltage per unit length versus heater power per unit length at a constant coil current. Also shown is the predicted curve using the theory in Section 2. The behavior is as expected, no voltage appears until a critical amount of heat has been supplied, beyond this the voltage rises gradually with heat input until all the current is driven into the substrate.

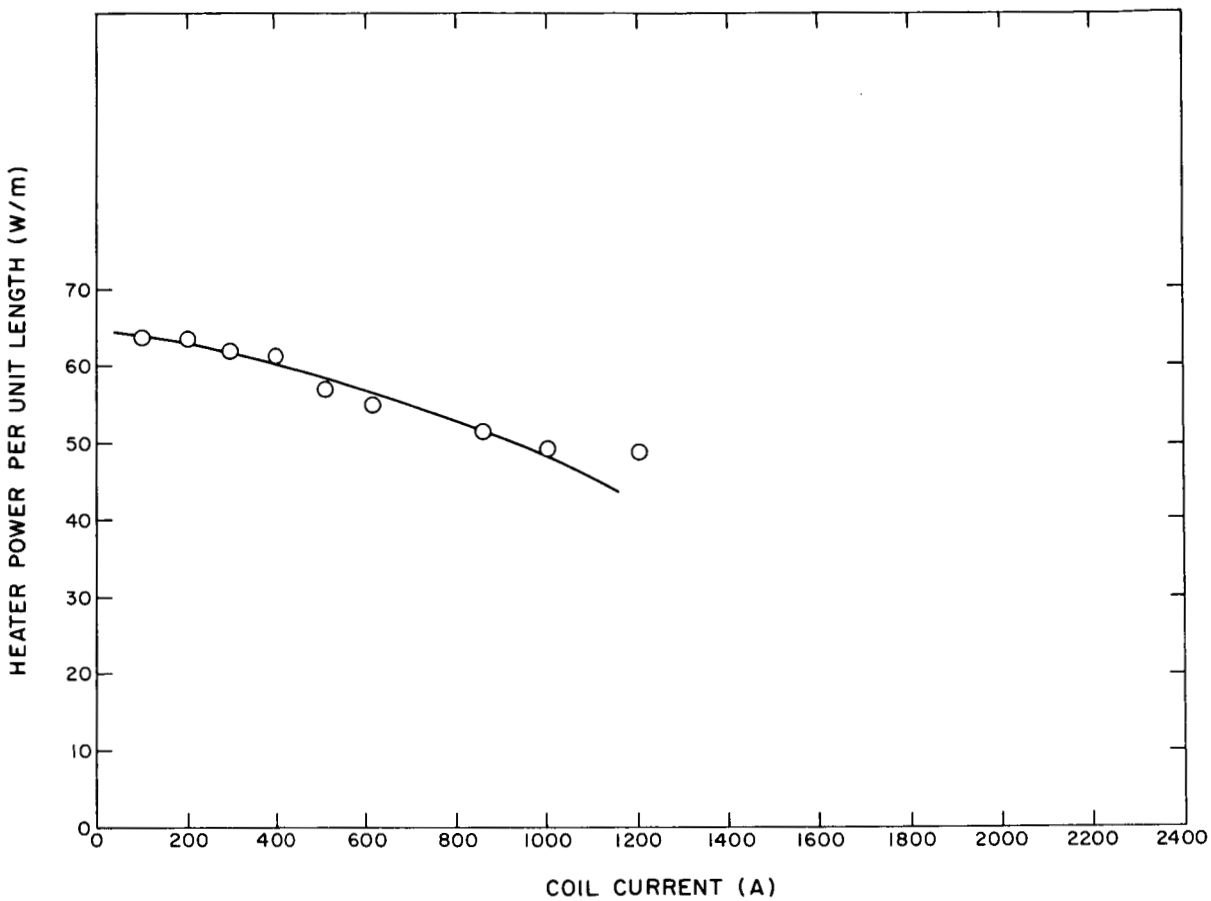

Fig. 27 Heater power at the onset of coil voltage plotted as a function of coil current. Extrapolation of this curve to zero heater power yields critical coil current.

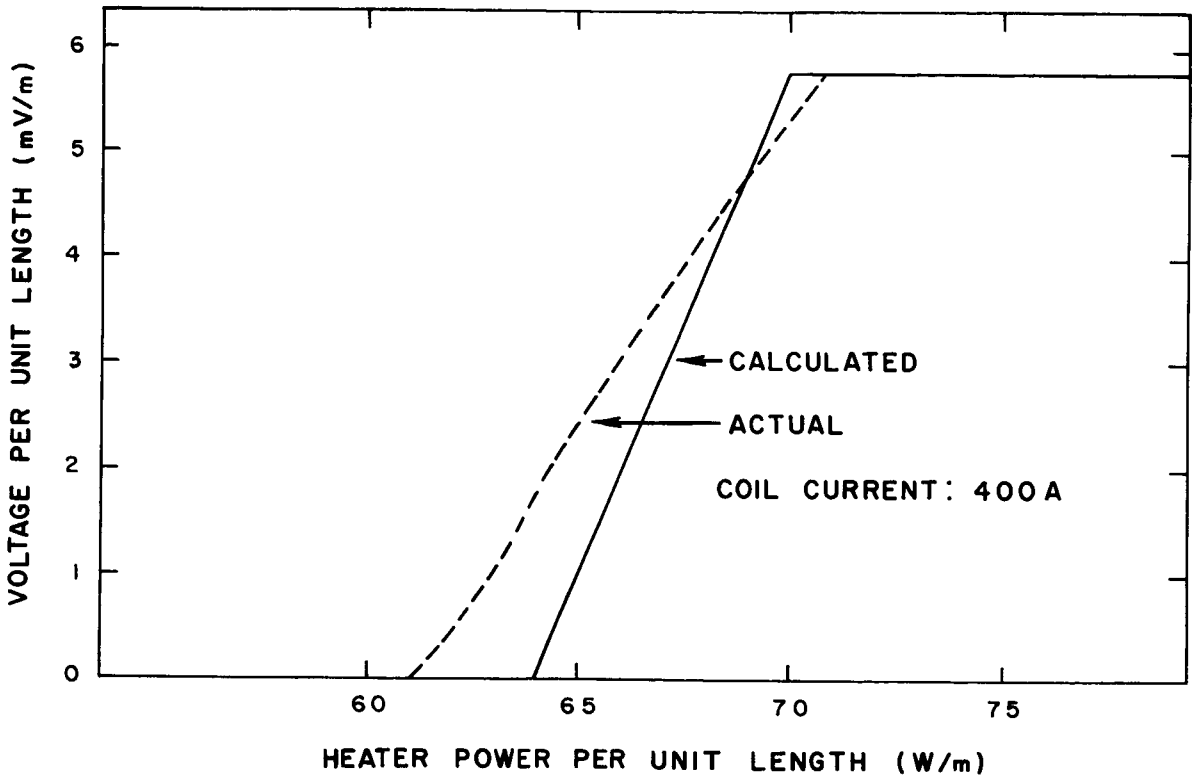

Fig. 28 Coil voltage response to heater power input for the 12.7 cm I.D. magnet.

VIII. CONCLUSION

The work outlined above represents successful solutions to the major obstacles encountered in using superconductors in strip form for the construction of large magnets. The section on stabilization outlines procedures whereby superconducting coils of any size and using any conductor cross section can be designed confidently from data contained only in short sample tests. In the remaining sections a discussion is presented of solutions to problems unique to strip type superconductors, and the performance of two actual solenoids is described.

While these two solenoids are in fact stable they are not optimally designed. Much remains to be investigated in terms of maximization of the overall current density, operation at temperatures other than 4.2°K and operation under partially stable or metastable conditions. The 12.7 cm I.D. magnet is instrumented for the purpose of implementing investigations of this type to further refine the technology of stabilization.

APPENDIX A

SURFACE CURRENT DISTRIBUTION ON AN INFINITELY CONDUCTIVE ELIPTIC CYLINDER

The function $z = c \sin w$ maps a semi-infinite slot of width π in the w plane as shown in Fig. A1 into the upper half of the z plane:

$$x = c \sin u \cos h v$$

$$y = c \cos u \sin h v$$

Lines of constant v in the w plane map as elipses of the form $x^2/c^2 \cos h^2 v + y^2/c^2 \sin h^2 v = 1$ in the z plane so that a rectangular strip of width π and thickness $\sin h^{-1} b/c$ in the w plane maps into a half elipse with major and minor axes a and b respectively in the z plane.

If we assume infinite conductivity and a potential ψ such that

$$H = -\nabla\psi = \frac{I}{2\pi} \tag{A1}$$

where I = total current in strip, then in the w plane the current density on the surface $v = v_o$ is uniform:

$$K = H - \frac{\partial\psi}{\partial u}\bigg|_{v = v_o} = \frac{I}{4\pi} \tag{A2}$$

In the z plane K is nonuniform and is given by:

$$K = H_s = -\frac{\partial\psi}{\partial s}\bigg|_{v = v_o} = \frac{I}{4\pi} \tag{A3}$$

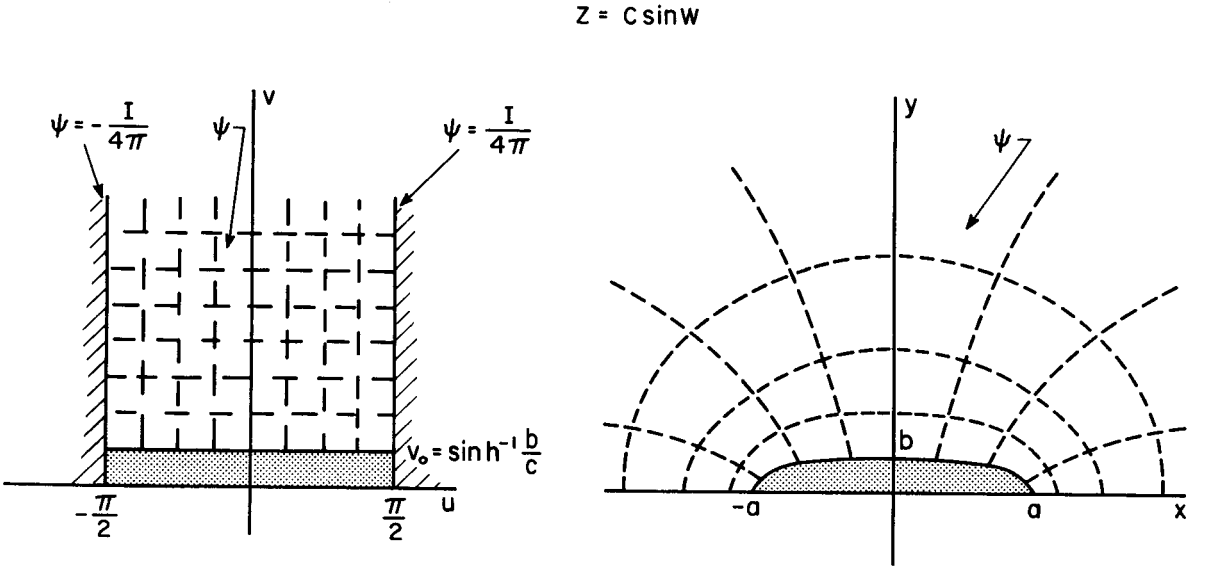

Fig. A1 The conformal transformation $z = c \sin w$.

where H_s = component of field parallel to strip and

$$ds = \sqrt{dx^2 + dy^2}$$

$$= c\sqrt{\cosh^2 v_o \cos^2 u + \sinh^2 v_o \sin^2 u}\, du$$

If we set $v_o = \sinh^{-1} b/c$ then

$$ds = \sqrt{a^2 \cos^2 u + b^2 \sin^2 u}\, du$$

so that

$$K = -\frac{\partial \psi}{\partial u}\frac{\partial u}{\partial s}\Bigg|_{v = v_o}$$

$$= \frac{I}{2\pi a}\left[-\frac{1}{\sqrt{\cos^2 u + \frac{b^2}{a^2}\sin^2 u}}\right] \qquad \text{(A4)}$$

The distance s along the surface of the strip is given by

$$s = \int_o^u ds \approx a \int_o^u \left[\cos u + \frac{b^2}{2a}\sin^2 u\right] du,$$

$$= a \sin u + \frac{b^2}{2a}\left[\frac{u}{2} - \frac{\sin u \cos u}{2}\right], \quad \frac{b}{a} \ll 1 \qquad \text{(A5)}$$

$$s_o = s\left(\frac{\pi}{2}\right) = a + \frac{\pi b^2}{8a} = a\left(1 + \frac{\pi b^2}{8a^2}\right)$$

$$\frac{S}{S_o} = \left[\frac{1}{1 + \frac{\pi b^2}{8a^2}}\right]\left[\sin u + \frac{b^2}{2a^2}\left(\frac{u}{2} - \frac{\sin u \cos u}{2}\right)\right] \qquad \text{(A6)}$$

The parameteric equations A4 and A6 in the parameter u form the basis for the plot shown in Fig. 12.

REFERENCES

1. A. R. Kantrowitz and Z. J. J. Stekly, "A New Principle for the Construction of Stabilized Superconducting Coils," Appl. Phys. Letters 6, 56, (1965).

2. R. D. Cummings and W. N. Latham, "An Experimental Measurement of the Dependence of the H-I Curve of Nb-Zr Wire on Temperature," Avco-Everett Research Laboratory, AMP 141, May 1964.

3. W. A. Little, M. A. LeBlanc, Proc. 7th Int. Conf. Low Temp. Physics, (1960). (University of Toronton Press, Toronto, 1961) p. 363.

4. B. S. Chandrasekhar, M. S. Walker, H. Riemersma, and F. E. Werner, Proc. 8th Int. Conf. Low Temp. Physics, (1962). (Butterworths, Washington, 1963) p. 345.

5. R. R. Hake, T. G. Berlincourt, and D. H. Leslie, IBM J. 6 (1962) 119.

6. T. G. Berlincourt, R. R. Hake, and D. H. Leslie, Phys. Rev. Ltrs. 6 (1961) 671.

7. R. R. Hake, D. H. Leslie, and T. G. Berlincourt, Phys. Rev. 127 (1962) 170.

8. M. S. Walker and M. J. Fraser, Superconductors. (Interscience, New York, 1962) p. 99.

9. C. S. Tedmon, Jr., R. M. Rose, and J. Wulff, Metallurgy of Advanced Electronics Materials. (Interscience, New York, 1962) p. 89.

10. D. Kramer and C. G. Rhodes, Metals 16 (1962) 90.

11. B. H. Heise, Linde Company, Tonawanda, N. Y. (unpublished).

12. Ethan Hoag, Experimental Investigation of Advanced Superconducting Magnets. Annual Report, Contract NAS 8-5279, September 1964.

13. Ethan D. Hoag, J. A. P. Vol. 36, No. 3 Part 2, p. 1183, March 1965.

14. Y. B. Kim, C. F. Hempstead, and A. R. Strnad, Phys. Rev. 129, 528 (1963).